REPORT 1233

CONTENTS

	Page
SUMMARY	683
INTRODUCTION	683
SHOCK INTERACTION OF SINGLE SHEAR WAVE	683
Qualitative Discussion	683
Quantitative Discussion	684
Elementary wave	684
Geometric reexamination of prior results	685
Initial shear wave (~ initial turbulence)	685
Refracted shear-entropy wave (~ final turbulence and entropy spottiness)	685
Generated sound wave (~ noise field)	686
Transformation to Cartesian coordinates	686
SPECTRAL ANALYSIS OF RANDOM FIELDS	686
Homogeneous Fields	687
Amplitude spectra	687
Correlations	687
Correlation and power spectra	687
Correlation spectrum in terms of amplitude spectra	687
Inhomogeneous Fields	688
Correlation of Two-Dimensional Field with Three-Dimensional Field	688
SHOCK INTERACTION OF SPECTRUM OF SHEAR WAVES (TURBULENCE)	689
Diagonal Terms of Velocity Spectrum Tensor	689
Turbulence field	689
Noise field	689
Mean-Square Velocity Components	689
Turbulence field	689
Noise field	689
Mean-Square Pressure	690
Mean-Square Temperature	690
Mean-Square Density	690
Correlations Not Jointly Involving Turbulence and Noise	690
Attempts at simplification	690
Cross-correlations	691
Correlations Between Turbulence and Noise	691
Interaction of Turbulence with an Oblique Shock	692
CALCULATIONS	692
Mean-Square Velocity Components in Turbulence Field	692
Mean-Square Temperature in Entropy Field	693
Mean-Square Pressure in Noise Field	693
RESULTS AND DISCUSSION	693
CONCLUDING REMARKS	695
APPENDIXES	695
A. SYMBOLS	695
B. COMPLETE VELOCITY SPECTRUM TENSORS	696
Turbulence field	696
Noise field	697
C. CALCULATIONS FOR AXISYMMETRIC INITIAL TURBULENCE	697
REFERENCES	698
TABLE	699

REPORT 1233

SHOCK-TURBULENCE INTERACTION AND THE GENERATION OF NOISE [1]

By H. S. Ribner

SUMMARY

The interaction of a convected field of turbulence with a shock wave has been analyzed to yield the modified turbulence, entropy spottiness, and noise generated downstream of the shock. This analysis generalizes the results of Technical Report 1164, which apply to a single spectrum component, to give the shock-interaction effects of a complete turbulence field. The previous report solved the basic gas-dynamic problem, and the present report has added the necessary spectrum analysis.

Formulas for spectra and correlations have been obtained and numerical calculations have been carried out to yield curves of root-mean-square velocity components, temperature, pressure, and noise in decibels against Mach number for the Mach number range of 1 to ∞; both isotropic and strongly axisymmetric (lateral perturbations/longitudinal perturbations ≈ 36/1) initial turbulence have been treated. It was found that in either case initial turbulence with a longitudinal component of 0.1 percent of stream velocity would yield a noise pressure level of about 120 decibels; the value of lateral component had relatively little effect.

The present results are applicable quantitatively to flow in ducts or channels containing normal shocks; they are presumed to provide a qualitative guide to the generation of noise by the shock structure in a supersonic free jet.

INTRODUCTION

The propulsion of aircraft by means of jets gives rise to intense noise as an unfortunate byproduct. Programs of noise abatement are under way, but at present they are largely empirical: even with the general guide provided by Lighthill's theory (ref. 1), the understanding of the mechanisms of noise generation is far from complete. It appears from both experimental and theoretical evidence, however, that the interaction of turbulence with shock waves must often play a part. On the theoretical side, the generation of noise by such interaction is pointed out independently in references 2 and 3. The shock-turbulence interaction was found to produce, in addition to the noise, an entropy "spottiness" aft of the shock (manifested as a temperature and density spottiness at constant pressure, ref. 2).

Turbulence, entropy spottiness, and noise (pressure fluctuations) are examples of the three fundamental modes of small disturbance perturbation of a gas (refs. 4 and 5): more specifically, the categories are vorticity mode, entropy mode, and sound mode. The vorticity mode (turbulence) and the entropy mode are essentially "frozen" patterns (to use Kovásznay's term) that are convected by the main flow; the sound mode, however, consists of waves that propagate in various directions in addition to being convected.

To the first order in the perturbation velocity, there is no tendency for the modes to interact or for an isolated mode to spontaneously generate one of the other modes (ref. 5). (The weak transference of turbulence into noise described by the Lighthill theory is a higher-order effect (ref. 1).) The presence of a shock wave, however, provides a mechanism for a very strong transference: thus, when any one of the three modes—turbulence, entropy spottiness, or noise—encounters a shock, the interaction will give rise to all three modes, in comparable strength, downstream of the shock (refs. 2, 4, and 6).

The first of these cases, shock-turbulence interaction, has been investigated at the NACA Lewis laboratory as an outgrowth of reference 2 and is reported herein. The analysis of the earlier paper was concerned with a single spectrum wave of a turbulent field and was primarily a study in gas dynamics. The present paper reformulates the results and incorporates them in a spectral analysis; from the analysis come the quantitative effects of the interaction of a convected homogeneous field of turbulence with an extended plane shock front. (Some results of this work are reported in abbreviated form in refs. 7 and 8.) The perturbation velocity, pressure, temperature, and density distributions behind the shock are described in terms of formulas for their spectra, correlations, and mean-square values; these are separated into the respective contributions of turbulence, entropy spottiness, and noise.

Numerical calculations are presented for the root-mean-square values of the pressure (noise) and components of the temperature and velocity perturbations for the Mach number range of 1 to ∞; one set of calculations refers to isotropic initial turbulence, another set to strongly axisymmetric initial turbulence (lateral perturbations/longitudinal perturbations ≈ 36/1). The noise pressure level is also presented on an acoustic scale for several levels of initial turbulence.

SHOCK INTERACTION OF SINGLE SHEAR WAVE

QUALITATIVE DISCUSSION

According to the Fourier integral theorem, a turbulent velocity field can be represented as a superposition or spectrum of elementary waves. A single spectrum wave can be interpreted physically as a plane sinusoidal wave of shear-

[1] Supersedes NACA TN 3255, "Shock-Turbulence Interaction and the Generation of Noise," by H. S. Ribner, 1954.

ing motion (e. g., ref. 9); a portion of such a wave is shown in perspective in sketch (a):

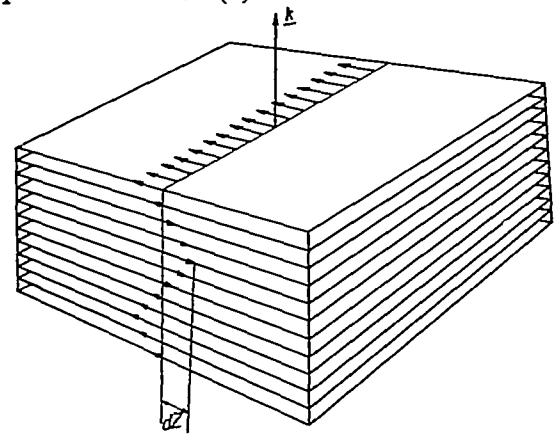

(a) Wave of shearing motion.

A similar wave encountering a shock is shown schematically in sketch (b),

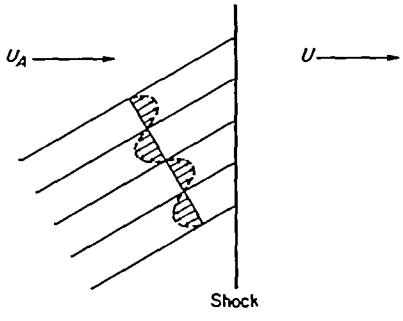

(b) Convection of shear wave through shock: original unsteady-flow problem.

the wave and the shock being viewed "edge-on." The wave-shock interaction is analyzed in reference 2, and what follows first is a brief physical account of the main results. The wave is supposed to be convected downstream by the mainstream with velocity U_A so that it passes through the shock. The passage is evidently an unsteady process, since the intercepts of the inclined lines—the planes of constant phase or wave fronts—move downward along the shock; it can be shown that a sinusoidal disturbance ripple will move along the shock with the same speed V.

The unsteady-flow problem may be treated directly (ref. 4), or it may be converted to an equivalent steady-flow problem by superposing an upward velocity V (ref. 2). The conversion is illustrated in sketch (c):

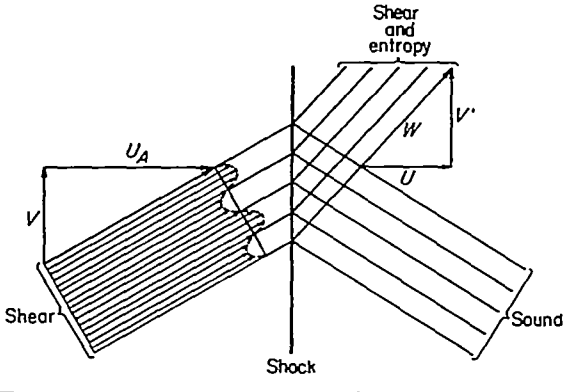

(c) Transformation to steady-flow problem by superposition of velocity V.

The cross velocity V therein has been chosen so that the resultant stream velocity is parallel to the wave fronts in the shear wave; the observer then sees what appears to be a steady sinusoidal shear flow passing through an oblique shock. This may be called the equivalent oblique shock. (Addition of the upward velocity V is, of course, equivalent to transforming to a moving frame of reference.)

Downstream of the shock, the resultant stream flow is deflected according to the laws for oblique shocks; the streamlines are the upper lines in the sketch. The vorticity of the initial shear wave is convected along these streamlines together with the additional vorticity generated by the shock. The net result is a refracted, amplified shear wave alined with these streamlines. The angle of refraction is just the angle of flow deflection of the oblique shock.

Superposed on the refracted shear wave is an entropy wave of the same inclination and wave length. This wave arises from the convection of entropy perturbations generated at the shock, precisely as the shear wave results from the convection of vorticity. The entropy wave is manifested physically as a spatial variation of temperature and density at constant pressure, by virtue of the equation of state.

The nonuniform velocity in the shear flow results in a nonuniform pressure jump across the shock. The ultimate effect is that the shock front develops ripples, modifying the pressure variations, and the resultant pressure variations propagate downstream as a plane sinusoidal wave (lower lines in sketch (c)).

The character of this wave depends on whether the resultant velocity W behind the equivalent oblique shock is subsonic or supersonic; this in turn depends on the initial wave inclination through V. When W is supersonic, the pressure wave is a plane sinusoidal sound wave; it appears as a stationary Mach wave pattern in the steady-flow reference frame. When W is subsonic, it may be shown that the pressure wave, while still plane, is not a simple sound wave, but rather attenuates exponentially with distance downstream of the shock; the resultant disturbance velocity is not normal to the wave front, and the wave propagates relative to the surrounding fluid at less than sonic speed.

QUANTITATIVE DISCUSSION

Elementary wave.—Thus far the waves have been discussed only qualitatively. Elementary spectrum waves of this sort may be expressed quantitatively in the form

$$d\alpha = dZ_\alpha e^{i\underline{k}\cdot\underline{x}} \tag{1}$$

(All symbols are defined in appendix A.) The wave-number vector $\underline{k}$ is directed normal to the wave fronts and its magnitude equals 2π/wave length. The wave amplitude is given by the complex quantity dZ_α. When α stands for temperature, pressure, density, or entropy, these are simple scalar waves. When α stands for the components u, v, w of the velocity, these are vector waves; two cases may then be distinguished: the waves are either irrotational and compressible (sound waves) or rotational and incompressible (vorticity waves). (See, e. g., ref. 10.) In the first case the irrotationality condition curl $\underline{\alpha}=0$ requires that the velocity $\underline{\alpha}$ and wave vector k be parallel (u, v, w proportional to k_1, k_2, k_3, respectively); the sound waves are thus longi-

tudinal. In the second case the incompressibility condition div $\underline{\alpha}=0$ requires that the velocity $\underline{\alpha}$ and the wave vector $\underline{k}$ be perpendicular; that is,

$$k_1u+k_2v+k_3w=0 \tag{2}$$

Thus, the vorticity waves are transverse and have the character of a shearing motion (see sketch (a)); in the discussion they have been referred to as "shear waves."

Geometric reexamination of prior results.—The shock-interaction process for a single shear wave is given quantitatively in reference 2, but the results are formulated in two dimensions. It will be necessary to reexamine the problem geometrically in order that the results may be reexpressed in three dimensions.

A perspective view of the initial shear wave in the new x_1, x_2, x_3-coordinate system is shown in figure 1. The portion of the shear wave shown is on the downstream side of the shock front, which is identified with the x_2, x_3-plane. A plane passed through the x_1-axis perpendicular to the wave fronts cuts the shock in the line Or. At a given instant of time this x_1, r-plane corresponds precisely to what is called the x, y-plane in reference 2. The angle φ of the x_1, r-plane with the horizontal is then the third coordinate in a system of cylindrical coordinates.

In reference 2 the time was eliminated from the equations by employing a frame of reference moving with a velocity V downward along the shock front, the so-called steady-flow frame of reference. In the present paper all results refer to a definite instant of time, $t=0$. Thus, motion of the reference frame plays no part, and the results of the earlier paper carry over to the present coordinate system on simply

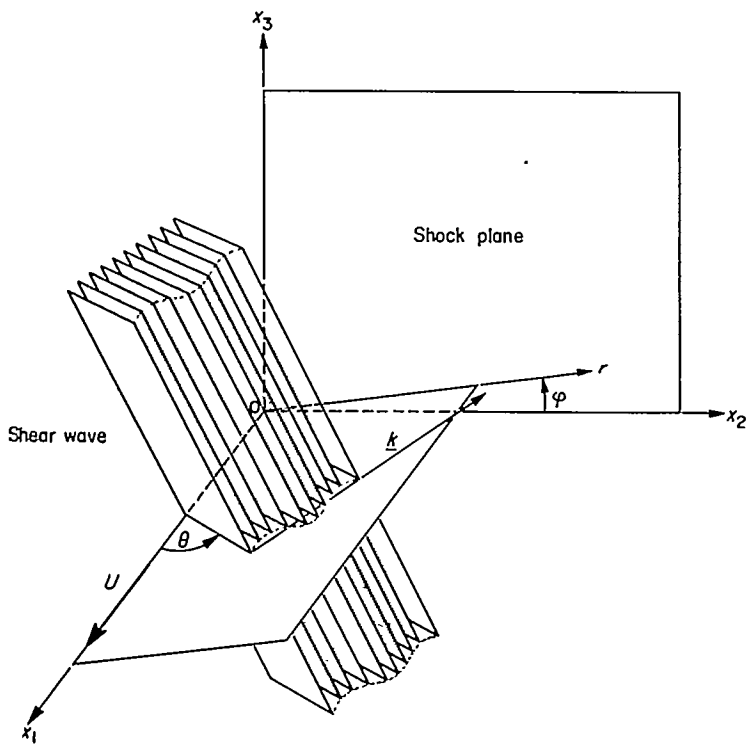

FIGURE 1.—Perspective view of shear wave in relation to reference frame.

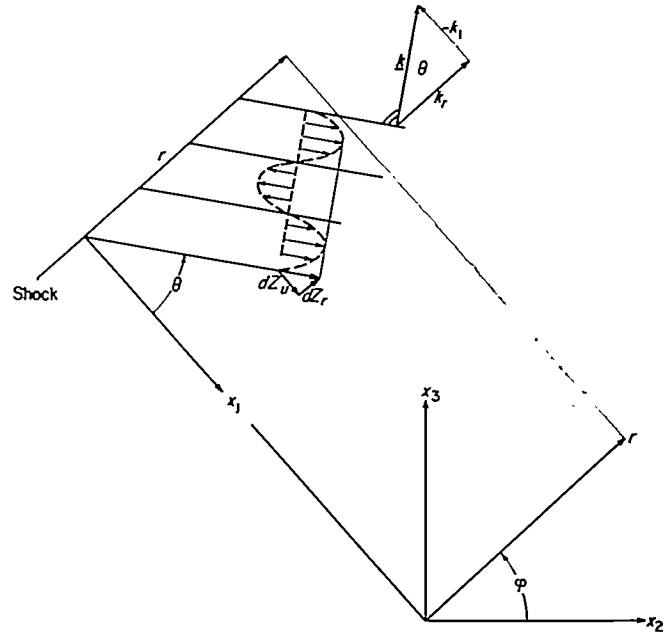

FIGURE 2.—Projective view of shear wave in relation to reference frame.

replacing x,y by x_1,r, respectively. The results of the transformation are given in the following sections with the disturbances reexpressed in nondimensional form according to the scheme

u, v, w=components of velocity perturbation/critical speed of sound a^*

p=pressure perturbation/mean static pressure

ρ=density perturbation/mean density

τ=temperature perturbation/mean temperature

In addition, there are other minor respects in which the notation has been modified from that of reference 2; for example, the waves are expressed in complex form.

Initial shear wave (~ initial turbulence).—At time $t=0$, the velocity field of the initial shear wave is, in cylindrical coordinates,

$$\left.\begin{aligned} du&=dZ_ue^{i\underline{k}\cdot\underline{x}}\\ dv_r&=dZ_re^{i\underline{k}\cdot\underline{x}}\\ dv_\varphi&=dZ_\varphi e^{i\underline{k}\cdot\underline{x}}\end{aligned}\right\} \tag{3}$$

where du is parallel to x_1 (longitudinal direction), dv_r is parallel to r, and dv_φ is perpendicular to r and x_1, in the direction of increasing φ (see figs. 1 and 2). The wave-number vector $\underline{k}$ lies in the x_1, r-plane, making an angle θ with the r-axis.

Refracted shear-entropy wave (~final turbulence and entropy spottiness).—The velocity field of the refracted shear wave (fig. 3) is

$$\left.\begin{aligned} du'&=dZ'_ue^{i\underline{k}'\cdot\underline{x}} & dZ'_u&=X\,dZ_u\\ dv'_r&=dZ'_re^{i\underline{k}'\cdot\underline{x}} & dZ'_r&=Y\,dZ_r\\ dv'_\varphi&=dZ'_\varphi e^{i\underline{k}'\cdot\underline{x}} & dZ'_\varphi&=dZ_\varphi\end{aligned}\right\} \tag{4}$$

at time $t=0$, where $\underline{k}'$ is the new wave-number vector, making an angle θ' with the r-axis. The radial components of $\underline{k}'$

and $\underline{k}$ are equal ($k_r'=k_r$), and the further dependence of $\underline{k}'$ on $\underline{k}$ is expressed through the dependence of θ' on θ. Similarly, the complex amplification factors X and Y depend on $\underline{k}$ in terms of θ. Expressions for X, Y, and θ' are given in appendix A.

The perturbation pressure dp' will be zero because this is again a shear wave, free of accelerations. The temperature perturbation associated with the companion entropy wave (fig. 3) will be

$$d\tau'=dZ_\tau' e^{i\underline{k}'\cdot\underline{x}} \qquad dZ_\tau'=\underline{T}\, dZ_u \tag{5}$$

With $p'=0$ (to the first order), the dimensionless density perturbation ρ' will be just the negative of the dimensionless temperature perturbation τ', according to the linearized equation of state. The form of the function $\underline{T}$ is given in appendix A.

Aside from the change in wave inclination, the description of the refracted shear-entropy wave in terms of the initial shear wave depends entirely on the amplification factors X and Y and the function T. Such functions play a role similar to the "transfer functions" of the theory of servomechanisms (ref. 11), and it appears appropriate to carry the name over to the present field.

Generated sound wave (~ noise field).—The shear-entropy wave downstream of the shock is accompanied by a plane irrotational pressure wave (sound wave) of different inclination (see fig. 3). For small inclinations θ of the initial shear wave, this pressure wave attenuates exponentially with distance from the shock; for inclinations greater than a certain critical value θ_{cr} (see appendix A), the pressure wave is unattenuated. The critical wave inclination θ_{cr} corresponds to the attainment of sonic speed in the mean flow behind the "equivalent oblique shock" referred to in the qualitative discussion.

The velocity field can be represented in the form

$$\left.\begin{aligned} du''&=dZ_u'' e^{i\underline{k}''\cdot\underline{x}} & dZ_u''&=\chi\, dZ_u \\ dv_r''&=dZ_r'' e^{i\underline{k}''\cdot\underline{x}} & dZ_r''&=\Upsilon\, dZ_u \\ dv_\varphi''&=dZ_\varphi'' e^{i\underline{k}''\cdot\underline{x}} & dZ_\varphi''&=0 \end{aligned}\right\} \tag{6}$$

where $\underline{k}''$ is the wave-number vector, making an angle θ'' with the r-axis; again the radial component matches that of $\underline{k}$; namely, $k_r''=k_r$. The sound-wave angle θ'' and the transfer functions χ and Υ are specified functions of the shear-wave angle θ; moreover, for $0\leq\theta<\theta_{cr}$, χ and Υ are functions of x_1, showing an exponential decay to zero as $x_1\rightarrow\infty$.

The pressure perturbation may be written

$$dp''=dZ_p'' e^{i\underline{k}''\cdot\underline{x}} \qquad dZ_p''=P\, dZ_u \tag{7}$$

where $P=P(x_1)$ is a transfer function defined in appendix A; like χ and Υ, P decays exponentially with x for $0\leq\theta<\theta_{cr}$. The corresponding density and temperature perturbations are proportional to p''; they may be obtained from the isentropic property of the sound wave as $\rho''=p''/\gamma$ and $\tau''=p''(\gamma-1)/\gamma$.

Transformation to Cartesian coordinates.—Expressions for the velocity field in Cartesian coordinates will be needed. The transformation from cylindrical coordinates is effected by means of the relations

$$\left.\begin{aligned} dZ_v&=dZ_r\cos\varphi-dZ_\varphi\sin\varphi \\ dZ_W&=dZ_r\sin\varphi+dZ_\varphi\cos\varphi \end{aligned}\right\} \tag{8}$$

where primes (~ refracted shear wave) or double primes (~ sound wave) may be inserted throughout as needed.

The transformation results in

$$\text{Initial shear}\left\{ d\alpha=dZ_\alpha e^{i\underline{k}\cdot\underline{x}},\ \text{where } \alpha=u, v, w \right\} \tag{9}$$

$$\text{Final Shear}\left\{\begin{aligned} &d\alpha'=dZ_\alpha' e^{i\underline{k}'\cdot\underline{x}},\ \text{where the values of } dZ_\alpha' \\ &\quad\text{for } \alpha=u, v, w \text{ are, respectively,} \\ &dZ_u'=X\, dZ_u \\ &dZ_v'=Y\, dZ_r\cos\varphi-dZ_\varphi\sin\varphi \\ &dZ_w'=Y\, dZ_r\sin\varphi+dZ_\varphi\cos\varphi \end{aligned}\right\} \tag{10}$$

$$\text{Sound}\left\{\begin{aligned} &d\alpha''=dZ_\alpha'' e^{i\underline{k}''\cdot\underline{x}},\ \text{where the values of } dZ_\alpha'' \\ &\quad\text{for } \alpha=u, v, w \text{ are, respectively,} \\ &dZ_u''=\chi\, dZ_u \\ &dZ_v''=\Upsilon\, dZ_r\cos\varphi \\ &dZ_w''=\Upsilon\, dZ_r\sin\varphi \end{aligned}\right\} \tag{11}$$

SPECTRAL ANALYSIS OF RANDOM FIELDS

The foregoing relations will be fitted later into a spectral analysis of the fields of turbulence and noise. Appropriate analytical techniques can be found in the spectral theory of random functions; suitable developments of this sort are given by, for example, Moyal (ref. 10) and Batchelor (ref. 12) for spatially homogeneous fields. The first part of the present section will be devoted to an interpretation (with some liberties) of relevant parts of the two papers; the latter part will be devoted to developments for inhomogeneous fields and for correlations of a two-dimensional field with a three-dimensional field.

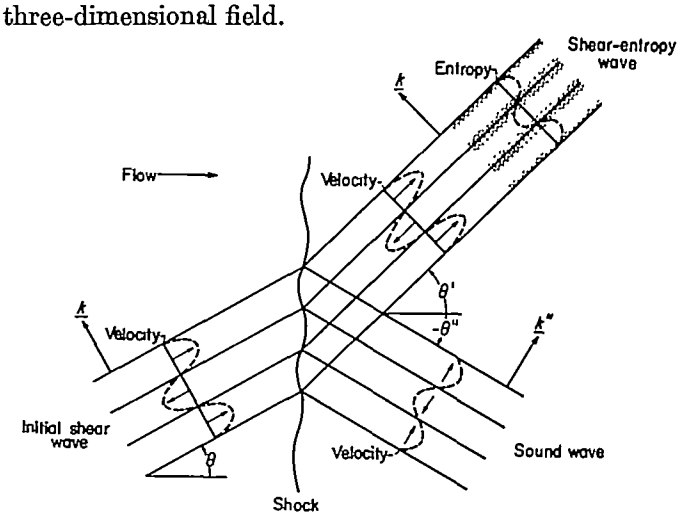

FIGURE 3.—Interaction of shear wave with shock: view in x_1, r-plane.

HOMOGENEOUS FIELDS

Amplitude spectra.—Consider a three-dimensional field of small disturbance (e. g., turbulence or noise) of unlimited extent. Let this field be homogeneous in the sense that the statistical properties do not vary from point to point. The instantaneous spatial distribution of any physical quantity α can then be represented mathematically by a Fourier integral in the Stieltjes form (refs. 10 and 12)

$$\alpha(\underline{x})=\int e^{i\underline{k}\cdot\underline{x}}dZ_\alpha(\underline{k}) \tag{12}$$

where the triple integral goes from $-\infty$ to ∞ in each component of $\underline{k}=(k_1, k_2, k_3)$.

If equation (12) is written in the form

$$\alpha=\int d\alpha(\underline{k})$$

then, by comparison with equation (1), $d\alpha$ can be identified with what has been called an elementary spectrum wave. The Fourier integral is thus to be interpreted as a superposition of infinitely many of such plane waves. In the integral the components of $\underline{k}$ take on all values; it follows from the significance of $\underline{k}$ as a wave-number vector that all wave inclinations and wave lengths appear. An aggregate of vorticity waves with a suitable distribution of amplitudes among the various wave lengths and inclinations can represent a turbulent field (ref. 13). Similarly, an aggregate of sound waves suitably distributed can represent a random noise field (ref. 10). Finally, an aggregate of the scalar entropy waves can represent a random field of entropy spottiness. A combination of these three basic types of disturbance—entropy spottiness, turbulence, and noise—constitutes the most general random small-disturbance field that may exist in a gas (refs. 4 and 5).

Correlations.—Let α be measured at some point P and β at some point $\hat{P}$ a vector distance $\underline{\xi}$ from P; then the space average of the product $\alpha\beta$ as $\hat{P}$ and P vary but their vector separation $\underline{\xi}$ is held fixed may be defined as the space-average correlation $\overline{\alpha\beta}(\underline{\xi})$. Alternatively, the disturbance field may be considered to be just one of a large number, or ensemble, of statistically similar fields (e. g., the flow fields of a great many "identical" wind tunnels operated simultaneously); the average of $\alpha\beta$, with P and $\hat{P}$ fixed, over all members of the group, is the ensemble-average correlation. The equations that follow, from the theory of random functions, refer solely to ensemble averages, but space averages are desired in practical applications. The ergodic hypothesis of probability theory equates the space average to the ensemble average provided that, at any instant, the disturbance fields α and β are stationary random functions of position; that is, the disturbance fields are spatially homogeneous.

In what follows, the term "cross-correlation" will be applied for $\alpha\neq\beta$, the term "self-correlation," or simply "correlation," for $\alpha=\beta$.

Correlation and power spectra.—The cross-correlation $\alpha\beta$ (ξ) (like α or β, indvidually: see eq. (12)) may be expressed by means of the Fourier integral as a spectrum of plane sine waves:

$$\overline{\alpha\beta}(\underline{\xi})=\int e^{i\underline{k}\cdot\underline{\xi}}[\alpha\beta]d\underline{k} \tag{13}$$

where $[\alpha\beta]$ is a function of $\underline{k}$, and $d\underline{k}$ is an abbreviation for $dk_1dk_2dk_3$. The differential $e^{i\underline{k}\cdot\underline{\xi}}[\alpha\beta]d\underline{k}$ may be regarded as the contribution to the correlation made by spectrum components with wave number between $\underline{k}$ and $\underline{k}+d\underline{k}$. The function $[\alpha\beta]$ is called the "spectral density" when $\alpha=\beta$, the "cross-spectral density" when $\alpha\neq\beta$ (ref. 11). The array of nine spectral densities signified by $[\alpha\beta]$ when α and β are limited to mean u, v, or w is the "spectral tensor" of the velocity field and is commonly written as Γ_{ij} of Φ_{ij}. (The corresponding array of the nine velocity correlations $\overline{\alpha\beta}(\underline{\xi})$ is the "correlation tensor," commonly written as $R_{ij}(\underline{\xi})$.)

Equation (13) includes as a special case the self-correlation or mean-square relation

$$\overline{\alpha^2}=\int[\alpha\alpha]d\underline{k}, \qquad \text{where } \xi=0 \tag{14}$$

If α were a velocity component (say u), then $\overline{\alpha^2}$ would be twice the space-average kinetic energy per unit mass associated with u. The spectral density $[\alpha\alpha]$ is in this case an energy density (per unit mass, per unit wave number). For similar reasons, where spectra of the kind defined by equation (14) have occurred in physics (e. g., in the harmonic analysis of radio noise), they have generally been called energy, intensity, or power spectra.

Correlation spectrum in terms of amplitude spectra.—The rather analogous forms of equations (12) and (13) are of interest. Equation (12) expresses the spectrum of the amplitude of the fluctuating quantity α; this may be termed an amplitude spectrum. Equation (13) expresses the spectrum of the correlation of α with β; this has been termed a correlation spectrum. The complex magnitude $dZ_\alpha(\underline{k})$ of the amplitude spectrum fluctuates in an apparently random manner as $\underline{k}$ is varied (refs. 10 and 12). The magnitude $[\alpha\beta]d\underline{k}$ of the correlation spectrum, on the other hand, varies smoothly with $\underline{k}$, since the correlation is a smoothed or averaged quantity (ref. 12). The amplitude spectrum gives no direct information concerning averaged (i. e., statistical) properties of the disturbance field, whereas the correlation spectrum leads directly to expressions for correlations and mean-square values (see eqs. (3) and (4)). One-dimensional spectra and scales of turbulence can also be determined (e. g., ref. 14).

It would be desirable to formulate the shock-turbulence interaction problem directly in terms of correlation spectra, but formidable difficulties stand in the way. It has been simpler to start with the shock interaction of a single shear wave, which deals with amplitude spectra, and to infer from this the changes in the correlation spectra. The whole procedure depends on the following relation (refs. 10 and 12) which connects the two kinds of spectra, namely,

$$[\alpha\beta]d\underline{k}=\overline{dZ_\alpha^*(\underline{k})dZ_\beta(\underline{k})} \tag{15}$$

where $dZ(\underline{k})$ is associated with the wave-number range between $\underline{k}$ and $\underline{k}+d\underline{k}$, and the bar represents the ensemble average. This relation is fundamental to the spectrum analysis of the present paper. Its significance is this: the single-wave analysis (summarized in an earlier section) provided the change in amplitude of an individual spectrum wave in the form $dZ_\alpha \rightarrow dZ'_\alpha$, say, and similarly, $dZ_\beta \rightarrow dZ'_\beta$; equation (15) provides the means for determining therefrom the corresponding change in the spectral density: $[\alpha\beta] \rightarrow [\alpha'\beta']$.

INHOMOGENEOUS FIELDS

The spectral representation of a spatially homogeneous random field is given by equation (12):

$$\alpha(\underline{x})=\int e^{i\underline{k}\cdot\underline{x}}dZ_\alpha(\underline{k})$$

A corresponding possible representation of an inhomogeneous field is

$$\alpha(\underline{x})=\int e^{i\underline{k}\cdot\underline{x}}dZ_\alpha(\underline{k},\underline{x}) \tag{16}$$

where dZ_α now depends on position; the sound field behind the shock is of this character. The following spectral analysis of such inhomogeneous fields is a development of Moyal's treatment of homogeneous fields (ref. 10).

Let $\alpha(\underline{x})$ and $\beta(\underline{x}')$ be inhomogeneous fields

$$\alpha(\underline{x})=\int e^{-i\underline{k}\cdot\underline{x}}dZ^*_\alpha(\underline{k},\underline{x}) \tag{17}$$

$$\beta(\underline{x}')=\int e^{i\underline{k}'\cdot\underline{x}'}dZ_\beta(\underline{k}',\underline{x}') \tag{18}$$

where equation (17) is an alternate form of equation (16). The correlation of α and β for fixed positions $\hat{\underline{x}}$ and $\hat{\underline{x}}'$, respectively, can be formed by taking the ensemble average of their product:

$$\overline{\alpha(\hat{\underline{x}})\beta(\hat{\underline{x}}')}=\overline{\iint e^{i(\underline{k}'\cdot\hat{\underline{x}}'-\underline{k}\cdot\hat{\underline{x}})}dZ^*_\alpha(\underline{k},\hat{\underline{x}})dZ_\beta(k',\hat{\underline{x}}')} \tag{19}$$

The operations of integration and averaging commute, so the averaging bar may be regarded as placed over the dZ's alone on the right side.

Equation (19) could immediately be simplified if the fields $\alpha(\underline{x})$ and $\beta(\underline{x}')$ were homogeneous; in that case the important relation

$$\overline{dZ^*_\alpha(\underline{k})dZ_\beta(\underline{k}')}=[\alpha\beta]d\underline{k}d\underline{k}'\delta(\underline{k}'-\underline{k}) \tag{20}$$

where

$$\delta(\underline{k}'-\underline{k})=0 \text{ for } \underline{k}'\neq\underline{k}$$
$$=\infty \text{ for } \underline{k}'=\underline{k}$$

and

$$\int_{-\infty}^{\infty}\delta(\underline{k}'-\underline{k})d\underline{k}'=1$$

would hold (ref. 10), according to the spectral theory of random functions. The simplification can still be achieved by replacing the inhomogeneous fields by "equivalent" homogeneous fields that match, respectively, at the points $\hat{\underline{x}}$ and $\hat{\underline{x}}'$. This is accomplished by freezing $dZ^*_\alpha(\underline{k},\underline{x})$ in equation (17) at the value $dZ^*_\alpha(k,\hat{\underline{x}})$ while allowing $\underline{x}$ to vary in the exponential, and correspondingly freezing dZ_β in equation (18).

When applied to the so-defined equivalent homogeneous fields, equation (20) reads

$$\overline{dZ^*_\alpha(\underline{k},\hat{\underline{x}})dZ_\beta(\underline{k}',\hat{\underline{x}}')}=\widehat{[\alpha\beta]}d\underline{k}d\underline{k}'\delta(\underline{k}'-\underline{k}) \tag{21}$$

where the $\frown$ over $[\alpha\beta]$ signifies the functional dependence on $\hat{\underline{x}}$ and $\hat{\underline{x}}'$. Upon substitution into equation (19) and integration over $\underline{k}'$ there results, with $\hat{\underline{\xi}}\equiv\hat{\underline{x}}'-\hat{\underline{x}}$,

$$\overline{\alpha(\hat{\underline{x}})\beta(\hat{\underline{x}}')}=\int e^{i\underline{k}\cdot\hat{\underline{\xi}}}\widehat{[\alpha\beta]}d\underline{k} \tag{22}$$

The spectral density $\widehat{[\alpha\beta]}$ can be evaluated by integrating equation (21) over $\underline{k}'$:

$$\widehat{[\alpha\beta]}d\underline{k}=\overline{dZ^*_\alpha(\underline{k},\hat{\underline{x}})dZ_\beta(\underline{k},\hat{\underline{x}}')} \tag{23}$$

where the integral property of the δ-function,

$$\int_{-\infty}^{\infty}f(\underline{k}')\delta(\underline{k}'-\underline{k})d\underline{k}'=f(\underline{k})$$

has been used, with $f(\underline{k}')$ an arbitrary function.

Equations (22) and (23) for inhomogeneous fields are of the same form as their counterparts, equations (13) and (15), respectively, for homogeneous fields. In the homogeneous case the dZ's are functions of position, and equation (23) mplies a corresponding dependence of $\widehat{[\alpha\beta]}$ on position. Moreover, the correlation $\overline{\alpha(\hat{\underline{x}})\beta(\hat{\underline{x}}')}$ depends on $\hat{\underline{x}}$ and $\hat{\underline{x}}'$ iseparately as well as on their separation $\hat{\underline{\xi}}$.

CORRELATION OF TWO-DIMENSIONAL FIELD WITH THREE-DIMENSIONAL FIELD

The local perturbations of the shock face from the mean (x'_2, x'_3) plane constitute a homogeneous two-dimensiona field of the general form

$$\beta(\hat{x}'_1, x'_2, x'_3)=\int e^{i(k'_2x'_2+k'_3x'_3)}dW_\beta(k'_2, k'_3) \tag{24}$$

where x'_1 has been fixed at the value $\hat{x}'_1$. It may be desired to correlate such a field locally with a three-dimensional field (e. g., the turbulent velocity field). To this end, equation (24) is rewritten in the form

$$\beta(\underline{x}')=\int e^{i\underline{k}'\cdot\underline{x}'}\left[e^{-k'_1x'_1}dW_\beta(k'_2, k'_3)\right]$$

Now, if x'_1 in $e^{-ik'_1x'_1}$ is fixed at the value $\hat{x}'_1$, β will be generalized to a three-dimensional field (elementary wave number $\underline{k}'$) that matches the original two-dimensional field in its

plane of definition $x_1=\hat{x}_1$. This "equivalent" field may be written

$$\left.\begin{aligned}\beta(\underline{x}')&=\int e^{i\underline{k}'\cdot\underline{x}'}\,dZ_\beta(\underline{k}')\\ \text{where}\qquad & \\ dZ_\beta(\underline{k}')&=e^{-ik_1'x_1'}\,dW_\beta(k_2',k_3')\end{aligned}\right\}\tag{25}$$

Equation (25) is of the form of a three-dimensional homogeneous field and may be used in place of (24) in equations (13) and (15) to provide the correlation of β with any three-dimensional homogeneous field in the common plane $x_1=\hat{x}_1$.

SHOCK INTERACTION OF SPECTRUM OF SHEAR WAVES (TURBULENCE)

The interaction of a single shear wave with a shock has been discussed in detail. With this as the basis, the statistical behavior of a spectrum of shear waves representing turbulence will now be derived; the procedure will make use of the spectral-analysis relations of the last section. The problem is formulated as follows: given the spectra (and hence correlations and mean-square values) associated with the turbulence convected into the shock, to calculate therefrom the spectra, correlations, and mean-square values associated with the turbulence, entropy spottiness, and noise in the flow downstream of the shock.

DIAGONAL TERMS OF VELOCITY SPECTRUM TENSOR

The respective spectrum tensors for the turbulence and noise downstream of the shock each consist of nine elements; of these the three diagonal terms are most important since they lead to the mean squares of the velocity components. The relatively simple derivation of the first diagonal term and the sum of the second and third will be carried out in the present section. The derivation of the complete tensor is carried out in appendix B by a more formal procedure.

Turbulence field.—The shock interaction effects have been expressed in terms of relations between wave amplitudes on opposite sides of the shock (eqs. (9) and (10)). Corresponding relations between spectral densities (elements) on the two sides can be obtained by use of equation (15). Some preliminary manipulation is required; thus multiply both sides of equations (10) by their complex conjugates, and add the last two; there results

$$dZ_u'^*dZ_u'=|X|^2dZ_u^*dZ_u \tag{26}$$

$$dZ_v'^*dZ_v'+dZ_w'^*dZ_w'=|Y|^2dZ_rdZ_r^*+dZ_\varphi^*dZ_\varphi \tag{27}$$

But by geometry (fig. 2),

$$dZ_r=dZ_u\tan\theta$$

$$dZ_r^*=dZ_u^*\tan\theta$$

and also, by the coordinate transformation (8),

$$dZ_r^*dZ_r+dZ_\varphi^*dZ_\varphi=dZ_v^*dZ_v+dZ_w^*dZ_w$$

Thus, equation (27) becomes

$$dZ_v'^*dZ_v'+dZ_w'^*dZ_w'=(|Y|^2-1)\tan^2\theta\,dZ_u^*dZ_u+dZ_v^*dZ_v+dZ_w^*dZ_w \tag{28}$$

Application of equation (15) yields

$$\left.\begin{aligned}[u'u']\,d\underline{k}'&=|X|^2\,[uu]\,d\underline{k}\\ \{[v'v']+[w'w']\}\,d\underline{k}'&=(|Y|^2-1)\tan^2\theta\,[uu]\,d\underline{k}+\{[vv]+[ww]\}\,d\underline{k}\end{aligned}\right\}\tag{29}$$

These are the desired expressions relating diagonal elements of the spectrum tensors of the turbulence on opposite sides of the shock.

Noise field.—If operations similar to those of the last section are applied to equations (11), there results

$$\left.\begin{aligned}[u''u'']\,d\underline{k}''&=|\chi|^2[uu]\,d\underline{k}\\ \{[v''v'']+[w''w'']\}\,d\underline{k}''&=|\Upsilon|^2\tan^2\theta\,[uu]\,d\underline{k}\end{aligned}\right\}\tag{30}$$

These equations relate the diagonal elements of the spectrum tensor of the noise generated behind the shock to the longitudinal spectral density of the initial turbulence ahead of the shock.[2]

MEAN-SQUARE VELOCITY COMPONENTS

Turbulence field.—The mean-square velocity components follow directly from integration of the spectral density (see eq. (14)). Integration of both sides of equations (29) yields

$$\left.\begin{aligned}\overline{u'^2}&=\int|X|^2[uu]\,d\underline{k}\\ \overline{v'^2}+\overline{w'^2}&=\overline{v^2}+\overline{w^2}+\int(|Y|^2-1)\tan^2\theta\,[uu]\,d\underline{k}\end{aligned}\right\}\tag{31}$$

Thus, the mean-square velocity components behind the shock (primed values) are given in terms of those ahead of the shock, the single-wave transfer functions X and Y, and the longitudinal spectral density $[uu]$ of the initial turbulence. Note that X and Y are functions of $\underline{k}$ in terms of θ (see appendix A).

Noise field.—Similarly, integration of equations (30) yields the mean-square velocity components in the noise field:

$$\left.\begin{aligned}\overline{u''^2}&=\int|\chi|^2\,[uu]\,d\underline{k}\\ \overline{v''^2}+\overline{w''^2}&=\int|\Upsilon|^2\tan^2\theta[uu]\,d\underline{k}\end{aligned}\right\}\tag{32}$$

Here again, χ and Υ are functions of k in terms of θ.

[2] Direct expressions for the spectra downstream of the shock may be desired, free of the unequal volume elements $d\underline{k}$, $d\underline{k}'$, or $d\underline{k}''$. This may be effected in eq. (29) by dividing both sides by $d\underline{k}'$; then (since $d\underline{k}$ is shorthand for $dk_1dk_2dk_3$, and similarly for $d\underline{k}'$) the ratio $d\underline{k}/d\underline{k}'$ may be interpreted as the Jacobian (say J') for the transformation from $\underline{k}$ to $\underline{k}'$. Upon evaluation,

$$J'=\frac{1}{m}$$

Similarly, in eq. (30) divide by $d\underline{k}''$ and interpret $d\underline{k}/d\underline{k}''$ as the Jacobian (say J'') for the transformation from $\underline{k}$ to $\underline{k}''$. Upon evaluation

$$J''=\frac{\cos^3\theta''}{m\cos^3\theta'}\frac{\partial\theta'}{\partial\theta''}$$

MEAN-SQUARE PRESSURE

The first-order pressure field is associated solely with the noise field: the pressure field associated with the turbulence is of the second order in velocity and may be neglected in comparison.[3] The spectral density of the noise pressure can be related to the spectral density of the longitudinal velocity in the initial turbulence; the relation is obtained by multiplying both sides of the second of equations (7) by their complex conjugates, averaging, and applying equation (15) to each side:

$$[p''p'']d\underline{k}''=|P|^2[uu]d\underline{k} \tag{33}$$

The integration of both sides of equation (33) yields the mean-square pressure in the noise field as

$$\overline{p''^2}=\int|P|^2[uu]d\underline{k} \tag{34}$$

MEAN-SQUARE TEMPERATURE

The temperature perturbations in the noise field, because of the isentropic relation, are equal to $(\gamma-1)/\gamma$ times the pressure perturbations; thus, the relations corresponding to equations (33) and (34) may be written down at once.

The temperature perturbations associated with the entropy spottiness behind the shock require a separate analysis. The spectral density of the temperature perturbations can be evaluated by operating on equation (5) in the now-familiar manner (see remarks preceding eq. (33)); the result is

$$[\tau'\tau']d\underline{k}'=|T|^2[uu]d\underline{k} \tag{35}$$

The integral relation obtained from equation (35) is

$$\overline{\tau'^2}=\int|T|^2[uu]d\underline{k} \tag{36}$$

This equation evaluates, for the region behind the shock, that part of the mean-square temperature spottiness associated with the entropy spottiness.

MEAN-SQUARE DENSITY

It is unnecessary to write down special expressions for the density field: the respective contributions of entropy spottiness and noise to the density perturbations are related to the corresponding temperature and pressure perturbations by $\rho'=-\tau'$ and ρ''/γ, according to the small-perturbation form of the equation of state.

CORRELATIONS NOT JOINTLY INVOLVING TURBULENCE AND NOISE

Attempts at simplification.—If the spectral density $[\alpha\beta](\underline{k})$ is known, the corresponding two-point correlation $\alpha\beta(\underline{\xi})$ can, in principle, be obtained by means of equation (13). In this fashion, for example, the longitudinal velocity correlation in the turbulence behind the shock may be expressed, with use of equation (29), as

$$\overline{u'u'}(\underline{\xi}')=\int|X|^2[uu]e^{i\underline{k}'\cdot\underline{\xi}'}d\underline{k} \tag{37}$$

or

$$=\int|X|^2[uu]e^{i\underline{k}'\cdot\underline{\xi}'}J'd\underline{k}' \tag{38}$$

(See footnote 2, p. 7, for significance of J'.)

Either of the forms (37) or (38) may prove awkward because of the admixture of $\underline{k}$ and $\underline{k}'$ in the integrand (e. g., $[uu]$ is ordinarily most simply expressed as a function of $\underline{k}$). However, it is possible to find a fixed vector $\underline{\xi}$ that satisfies the relation $\underline{k}'\cdot\underline{\xi}'=\underline{k}\cdot\underline{\xi}$; this gives the more convenient relation

$$\overline{u'u'}(\underline{\xi}')=\int|X|^2[uu]e^{i\underline{k}\cdot\underline{\xi}}d\underline{k} \tag{39}$$

where $\xi_1=m\xi_1'$, $\xi_2=\xi_2'$, $\xi_3=\xi_3'$. In all the self- or cross-correlations involving properties of the turbulence and entropy spottiness behind the shock, whether they be velocity components, temperature, density, or entropy, the transformation $k'\cdot\underline{\xi}'=\underline{k}\cdot\underline{\xi}$ can be made to simplify the exponential.

The physical interpretation of the relation between $\underline{\xi}$ and $\underline{\xi}'$ is this: if two fluid particles upstream of the shock are a vector distance $\underline{\xi}$ apart, after convection through the shock they will be a vector distance $\underline{\xi}'$ apart. Put another way, a "box" of turbulent fluid of edges ξ_1, ξ_2, ξ_3 will be compressed on passing through the shock and will emerge downstream as a shorter box of edges ξ_1', ξ_2', ξ_3'. Therefore, equation (39) in effect expresses correlations in the space downstream of the shock in terms of equivalent correlations in a stretched space upstream of the shock.

The analog of equation (37) for the correlations of properties of the noise field involves $\underline{k}''\cdot\underline{\xi}''$ in the exponential, rather than $\underline{k}'\cdot\underline{\xi}'$. Here no great simplification appears to be possible in general:[4] there exists no *fixed* vector ξ that satisfies the relation $\underline{k}''\cdot\underline{\xi}''=\underline{k}\cdot\underline{\xi}$. This lack reflects the nature of the transformation from $\underline{k}$ to $\underline{k}''$: the respective components of the two vectors are not in fixed proportions, but instead vary with the inclination of $\underline{k}$. The particular coordinate compression $\underline{\xi}\rightarrow\underline{\xi}'$ that works for the turbulent field (it expresses the change in dimensions of a fluid "box" convected through the shock) will not work for the noise field. An exception occurs when $\underline{\xi}''$ is chosen parallel to the shock plane (radial direction, $x_1=0$). Then $\underline{k}''\cdot\underline{\xi}''=k_r''\xi''$, and since $k_r''=k_r$, it follows that for this case $\underline{k}''\cdot\underline{\xi}''=\underline{k}\cdot\underline{\xi}''$.

The integral for a particular correlation simplifies considerably when $\underline{\xi}$ (or $\underline{\xi}'$, or $\underline{\xi}''$) is taken in the direction of one

[3] The local pressure field associated with turbulence, although weak by aerodynamic standards, may be strong by acoustic standards. If the turbulence (e. g., in a boundary layer) is convected past a stationary microphone, a strong response can be observed; the phenomenon is called "pseudo-sound." The noise sensation produced by wind blowing past the ears is presumably a similar effect associated with turbulent separation of the flow.

[4] A partial simplification is $\underline{k}''\cdot\underline{\xi}''=\underline{k}\cdot\underline{\xi}''+(k_1'-k_1)\xi_1''$.

of the coordinate axes, say x_i. In the former case, $\underline{k}\cdot\underline{\xi}$ becomes $k_i\xi$; and the exponential can be replaced by cos $k_i\xi$, since the imaginary sine component will integrate out. Similarly $e^{i\underline{k}''\cdot\underline{\xi}''}$ can be replaced by cos $k_i''\xi''$.

Cross-correlations.—The phase angles of the transfer functions must be considered in formulating cross-correlations. For example, the correlation of local temperature with longitudinal velocity in the entropy and turbulence fields behind the shock is readily obtained as

$$\overline{\tau'u'}(0)=\int (Te^{i\delta_T})^*(Xe^{i\delta_s})[uu]d\underline{k}$$

$$=\int TXe^{i(\delta_s-\delta_T)}\,[uu]\,d\underline{k}$$

The integrand, except for the exponential, is even in the wave inclination θ; the phase angles δ_s and δ_T (in the notation used) are odd in θ (both properties can be inferred from the symmetry of the wave-refraction process with respect to θ). Accordingly, the imaginary sine term in the exponential will integrate out, and

$$\overline{\tau'u'}(0)=\int TX\cos(\delta_s-\delta_T)[uu]d\underline{k} \tag{40}$$

The corresponding relations for other cross-correlations can be written down by analogy.

CORRELATIONS BETWEEN TURBULENCE AND NOISE

Cross-correlations between the turbulence and noise fields require a special treatment, partly because of the inhomogeneity of the noise field, and partly because of the nonparallelism of the physically associated waves. In what follows, an expression for the correlation of noise pressure with longitudinal turbulent velocity will be derived. From this the qualitative variation of the correlation with distance downstream of the shock will be inferred.

The refracted shear wave ($\sim\underline{k}'$) and pressure wave ($\sim\underline{k}''$) associated in an elementary interaction process have different inclinations (fig. 3). As a consequence, the formal application of the relations given in the section **SPECTRAL ANALYSIS OF RANDOM FIELDS** leads to difficulty: the spectral density of any correlation appears to vanish according to equation (21). Actually, the formulas are inapplicable to correlations involving mutually inclined waves; this will be brought out clearly in the following derivation of the applicable formulas. For simplicity the derivation will be limited to the correlation of turbulent longitudinal velocity u' at point $\underline{x}'$ with noise pressure p'' at point $\underline{x}''$; extensions to other cases are straightforward. The derivation will first be carried out as though the noise field were homogeneous (no variation of transfer function P with $\underline{x}$), and then will be adapted to take account of the actual inhomogeneity.

The respective Fourier integrals may be written

$$u'(\underline{x}')=\int e^{i\underline{k}'\cdot\underline{x}'}dZ_u(\underline{k}')=\int e^{-i\underline{k}'\cdot\underline{x}'}dZ_u^*(\underline{k}')$$

$$p''(\underline{x}'')=\int e^{i\hat{\underline{k}}''\cdot\underline{x}''}dZ_p(\hat{\underline{k}}'')$$

The correlation may be formed as the ensemble average of the product $u'p''$:

$$\overline{u'(\underline{x}')p''(\underline{x}'')}=\iint e^{i(\hat{\underline{k}}''\cdot\underline{x}''-\underline{k}'\cdot\underline{x}')}\overline{dZ_u^*(\underline{k}')dZ_p(\hat{\underline{k}}'')} \tag{41}$$

where the bar has been taken inside the integral, since the operations of averaging and integration commute. Equation (7) and the first of equations (4) may be used to simplify the right side:

$$\overline{dZ_u^*(\underline{k}')dZ_p(\hat{\underline{k}}'')}=X^*(\underline{k})P(\hat{\underline{k}})\overline{dZ_u^*(\underline{k})dZ_u(\hat{\underline{k}})} \tag{42}$$

where $\hat{\underline{k}}''$ bears the same relation to $\hat{k}$ as $\underline{k}''$ does to $\underline{k}$. By virtue of equation (20), equation (42) reduces further to

$$\overline{dZ_u^*(\underline{k}')dZ_p(\hat{\underline{k}}'')}=X^*(\underline{k})P(\hat{\underline{k}})[uu]\delta(\hat{\underline{k}}-\underline{k})d\underline{k}\,d\hat{\underline{k}}$$

if the fields are homogeneous. Substitution of this relation into equation (41) and integration over $\hat{\underline{k}}$ result in

$$\overline{u'(\underline{x}')p''(\underline{x}'')}=\int e^{i(\underline{k}''\cdot\underline{x}''-\underline{k}'\cdot\underline{x}')}X^*(\underline{k})P(\underline{k})[uu]d\underline{k} \tag{43}$$

since the δ-function eliminates all values of $\hat{\underline{k}}$ but $\underline{k}$ and similarly all values of $\hat{\underline{k}}''$ but $\underline{k}''$. Finally, the equation may be generalized to apply to the actual inhomogeneous pressure field, according to equation (23) and the discussion preceding it, by writing $P(\underline{k})$ as $P(\underline{k}, x_1'')$ and using the value appropriate to x_1''.

Equation (43) is the general relation for the two-point correlation of longitudinal turbulent velocity u' with noise pressure p''. The striking feature is the difference of the exponential term from those in equations (13) and (22); this constitutes an a posteriori demonstration of the inapplicability of those equations.[5]

If the turbulent velocity and noise pressure are correlated locally ($x''=x'$), the expression simplifies to

$$\overline{u'p''}(\underline{x}')=\int e^{i(k_1''-k_1')x_1'}X(\underline{k})P(\underline{k}, x_1')[uu]d\underline{k} \tag{44}$$

since $k_2''=k_2'$, $k_3''=k_3'$. Directly at the shock, $x_1'=0$ and the right side simplifies further; the integration can readily be carried out for isotropic turbulence, and a nonvanishing correlation will be obtained. Behind the shock ($x_1'>0$), the exponential oscillates sinusoidally; for a given wave inclination the behavior is essentially like cos Ckx_1', where C is a constant. For x_1' very small, the cosine is near unity over the significant range of k (the range for which $[uu]\gg 0$). Hence the correlation is only slightly diminished at small distances behind the shock. At somewhat greater distances the oscillatory nature of the cosine begins to be felt before $[uu]$ dies out, and the correlation falls off noticeably. Finally, at very large distances, cos Ckx_1' oscillates over a great

[5] However, eq. (43) is equivalent to that which would result from eq. (13) or (22) upon replacing the pressure wave by a locally equivalent shear wave parallel to the actual shear wave, as discussed in ref. 8.

many periods as k covers its important range, and the plus and minus contributions to the integral cancel each other; thus at these large distances behind the shock the noise-turbulence correlation falls to zero.

INTERACTION OF TURBULENCE WITH AN OBLIQUE SHOCK

All the foregoing analysis may be applied to an oblique shock by treating the latter as a normal shock with a superposed cross-velocity which is to be ignored. The coordinate system should be oriented so that the x_1-axis is normal to the oblique-shock front (on the downstream side), and the x_2- and x_3-axes lie in the shock front with the x_3-axis in the plane of the stream-velocity vector and the x_1-axis. The component of the stream velocity in the x_1-direction is the U velocity of the equivalent normal shock. From here on the analysis for the normal-shock case may be applied.

Ordinarily the turbulence spectrum tensor will be defined (as Φ'_{ij}, say) in a system x'_1, x'_2, x'_3 with the x'_1-axis alined with stream direction, and it will be necessary to transform Φ'_{ij} to the new system x_1, x_2, x_3. If the shock angle of the oblique shock is ψ, the primed and unprimed axes are related according to the following scheme:

	x_1	x_2	x_3
x'_1	$r_{11}=\sin\psi$	$r_{12}=0$	$r_{13}=\cos\psi$
x'_2	$r_{21}=0$	$r_{22}=1$	$r_{23}=0$
x'_3	$r_{31}=-\cos\psi$	$r_{32}=0$	$r_{33}=\sin\psi$

(45)

where r_{ij} is the cosine of the angle between x'_i and x_j. The transformation is effected by the formula

$$\Phi_{mn}=r_{im}r_{jn}\Phi'_{ij} \tag{46}$$

where the repeated indices i and j are to be summed over. The diagonal terms in the result are relatively simple:

$$\left.\begin{aligned}\Phi_{11}&=\Phi'_{11}\sin^2\psi+\Phi'_{33}\cos^2\psi-\sin\psi\cos\psi\,(\Phi'_{13}+\Phi'_{31})\\ \Phi_{22}&=\Phi'_{22}\\ \Phi_{33}&=\Phi'_{11}\cos^2\psi+\Phi'_{33}\sin^2\psi+\sin\psi\cos\psi\,(\Phi'_{13}+\Phi'_{31})\end{aligned}\right\} \tag{47}$$

The coordinate transformation whereby Φ'_{ij} goes over into Φ_{mn} may be illustrated most simply by choosing Φ'_{ij} to correspond to isotropic turbulence; in that case, Φ'_{ij} has the general form (e. g., ref. 12)

$$\Phi'_{ij}=F(k')(k'^2\delta_{ij}-k'_ik'_j) \tag{48}$$

Substitution into the first of equations (47) yields

$$\begin{aligned}\Phi_{11}&=F(k')\,[(k'^2_2+k'^2_3)\sin^2\psi+(k'^2_2+k'^2_1)\cos^2\psi+2k'_1k'_3\sin\psi\cos\psi]\\ &=F(k')\,[k'^2_2+(k'_3\sin\psi+k'_1\cos\psi)^2]\end{aligned} \tag{49}$$

In the preceding equations, k'_1, k'_2, k'_3 are the components of the wave-number vector in the primed coordinate system; these are related to the components k_1, k_2, k_3 in the unprimed system precisely as x'_1, x'_2, x'_3 are related to x_1, x_2, x_3 in equations (45). As a consequence, equation (49) can be readily shown to reduce to

$$\Phi_{11}=F(k)\,[k^2_2+k^2_3] \tag{50}$$

The corresponding element of equation (48) is

$$\Phi'_{11}=F(k')\,[k'^2_2+k'^2_3] \tag{51}$$

Thus the tensor elements Φ_{11} and Φ'_{11} have the same functional form, reflecting the isotropic property of invariance under rotation of coordinates. This particular example of the coordinate rotation applied to isotropic turbulence is trivial in that the result could have been written down in advance without recourse to the transformation equation. Nevertheless, it illustrates the formal application of the transformation and, in addition, serves as a check on the first of equations (47) in yielding the required invariance.

CALCULATIONS

Numerical calculations have been carried out for flows in which the turbulence incident on the shock is (1) isotropic and (2) strongly axisymmetric. An account of the isotropic case follows. The more complicated axisymmetric case adds little of interest and is therefore left to appendix C.

MEAN-SQUARE VELOCITY COMPONENTS IN TURBULENCE FIELD

The equations that jointly relate the upstream (unprimed) and downstream (primed) mean squares are

$$\overline{u^2}=\int[uu]\,d\underline{k} \tag{52}$$

$$\overline{u'^2}=\int|S|^2\frac{\cos^2\theta'}{\cos^2\theta}\,[uu]\,d\underline{k} \tag{53}$$

$$\overline{v'^2}+\overline{w'^2}=\int|S|^2\frac{\sin^2\theta'-\sin^2\theta}{\cos^2\theta}\,[uu]\,d\underline{k}+\overline{v^2}+\overline{w^2} \tag{54}$$

The first of these is just equation (14) with $\alpha=u$; the last two result from substituting into equations (31) the expressions for $|X|^2$ and $|Y|^2$ from appendix A. So far the equations have not been specialized to isotropic initial turbulence.

When the initial turbulence is isotropic (i. e., has spherical symmetry), its longitudinal spectral density $[uu]$ has the general form (e. g., ref. 12, eq. (3.4.12))

$$[uu]=k^2F(k)\cos^2\theta \tag{55}$$

where $F(k)$ is an arbitrary function of k. ($F(k)$ will ultimately cancel out in forming ratios.) It is appropriate, then, to go over to a form of spherical polar coordinates:

$$\left.\begin{aligned}k_1&=-k\sin\theta\\ k_2&=k\cos\theta\cos\varphi\\ k_3&=k\cos\theta\sin\varphi\\ d\underline{k}&=k^2\cos\theta\,dk\,d\varphi\,d\theta\end{aligned}\right\} \tag{56}$$

Equations (52) and (53) may now be written

$$\overline{u^2}=2\int_0^\infty k^4F(k)\,dk\int_0^{2\pi}d\varphi\int_0^{\pi/2}\cos^3\theta\,d\theta \tag{57}$$

$$\overline{u'^2}=2\int_0^\infty k^4F(k)\,dk\int_0^{2\pi}d\varphi\int_0^{\pi/2}|S|^2\cos^2\theta'\cos\theta\,d\theta \tag{58}$$

where the factor of 2 and the limit $\pi/2$ result from the sym-

metry in θ. Division of equation (58) by (57) yields, since $\int_0^{\pi/2} \cos^3\theta\, d\theta = 2/3$,

$$\overline{u'^2}/\overline{u^2} = \frac{3}{2}\int_0^{\pi/2} |S|^2 \cos^2\theta' \cos\theta\, d\theta \tag{59}$$

In a rather similar fashion, equation (36) yields

$$\overline{v'^2}/\overline{u^2} = \overline{w'^2}/\overline{u^2} = \frac{3}{4}\left(1 + \int_0^{\pi/2} |S|^2 \sin^2\theta' \cos\theta\, d\theta\right) \tag{60}$$

where use has been made of the initial isotropy $\overline{u^2} = \overline{v^2} = \overline{w^2}$, and final axisymmetry $\overline{v'^2} = \overline{w'^2}$.

The transfer function S in equations (59) and (60) is a measure of the amplification of a single spectral component in passing through the shock; the associated phase angle is δ_s (not relevant here). S, like the other transfer functions, is a complicated function of θ that does not lend itself to analytic integration. A numerical tabulation of S and δ_s against θ is given in tables I (c) to (k) for the respective Mach numbers of 1.10, 1.25, 1.5, 2.0, 2.5, 3.0, 4.0, 6.0, and ∞; these tables were used in conjunction with numerical integration to evaluate equations (57) and (58). (S reduces to 1 for all θ at $M=1$.)

MEAN-SQUARE TEMPERATURE IN ENTROPY FIELD

The derivation of $\overline{\tau'^2}/\overline{u^2}$ is parallel to that of $\overline{u'^2}/\overline{u^2}$, equation (53) being replaced by equation (36). The result is (analog of eq. (59)):

$$\overline{\tau'^2} = \frac{3}{2}\overline{u^2}\int_0^{\pi/2} |T|^2 \cos^3\theta\, d\theta \tag{61}$$

The transfer function T and the associated phase angle δ_T (not relevant here) are tabulated against θ in tables I (c) to (k) for the various Mach numbers. The tabulated values used in the numerical integration of equation (61).

MEAN-SQUARE PRESSURE IN NOISE FIELD

Because of the similarity of equations (34) and (36), the mean-square pressure can be written down by inspection of equation (61):

$$\overline{p''^2} = \frac{3}{2}\overline{u^2}\int_0^{\pi/2} |P|^2 \cos^3\theta\, d\theta \tag{62}$$

The integration has been performed numerically with use of the definition of P in terms of Π (appendix A) and the values of Π against θ tabulated in tables I (a) to (i), appropriate to $x=\infty$. Thus, the integral as evaluated refers to the asymptotic mean-square pressure far behind the shock.

RESULTS AND DISCUSSION

The results of the calculations of the preceding section are shown in figure 4 for Mach numbers of 1 to ∞; this figure evaluates the disturbance field—both turbulence and noise—downstream of a shock when isotropic turbulence is convected into the shock. The velocity perturbations, on a root-mean-square basis, are in percent of stream velocity *ahead* of the shock (thus the basis is the same on both sides of the shock); the temperature and pressure perturbations are in percent of ambient *behind* the shock.[6] The velocity curves refer solely to the turbulence component, the temperature curve to the entropy component, and the pressure curve to the noise component of the field behind the shock.

The curves show that isotropic turbulence is somewhat transformed in passing through a shock, the longitudinal and lateral components no longer being equal; the selective effect is, however, mild compared with that of screens or wind-tunnel contractions (cf., e. g., ref. 14). In addition, although the incident flow was assumed isothermal and isentropic, the downstream flow possesses an entropy spottiness, which is a "frozen" convected pattern like the turbulence. The root-mean-square temperature associated with the entropy spottiness, in percent of ambient, is seen to be not much less than the root-mean-square velocity of the initial turbulence, in percent of free stream.

In the theory the entropy spottiness is spatially correlated with the longitudinal component of the turbulent velocity everywhere behind the shock. In practice it is to be expected that the correlation will soon be destroyed by eddy intermixing as the combined fields are convected downstream from the shock; this intermixing, being second order, is neglected in the linear theory. Directly at the shock, the noise pressure likewise is correlated with the longitudinal component of the turbulent velocity. According to the earlier qualitative examination, however, this correlation falls off with distance behind the shock, reaching zero far back.

The peculiar hump in the curve of root-mean-square noise pressure against Mach number just above $M=1$ has commanded special attention. In order to delineate the shape accurately, additional numerical computations (beyond those for the other curves) were made at $M=1.05$ and $M=1.01$. These were supplemented by an analytical study which established that the curve varies like $(M-1)^{1/4}$ as $M\to 1$

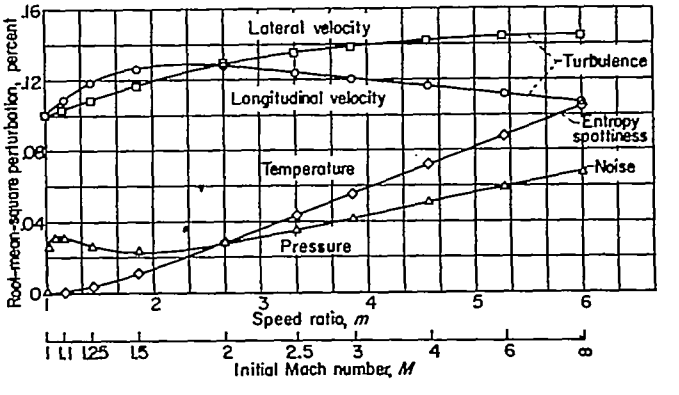

FIGURE 4.—Disturbances produced behind shock by interaction with isotropic turbulence. Turbulent intensity just before shock, 0.1 percent. Root-mean-square velocity in percent of initial stream velocity ahead of shock; root-mean-square temperature and pressure in percent of ambient behind shock.

[6] For the circumstances of figs. 4 and 5, namely, longitudinal component of initial turbulence equals 0.1 percent of stream velocity, the dimensional quantities plotted are as follows in terms of the nondimensional symbols used in the analysis: longitudinal velocity, percent initial stream velocity, 0.1 $\sqrt{\overline{u'^2}/\overline{u^2}}$; lateral velocity, percent initial stream velocity, 0.1 $\sqrt{\overline{v'^2}/\overline{u^2}}$; temperature, percent ambient, 0.1 $\sqrt{\overline{m\tau'^2}/\overline{u^2}}$; pressure, percent ambient, 0.1 $\sqrt{\overline{mp''^2}/\overline{u^2}}$.

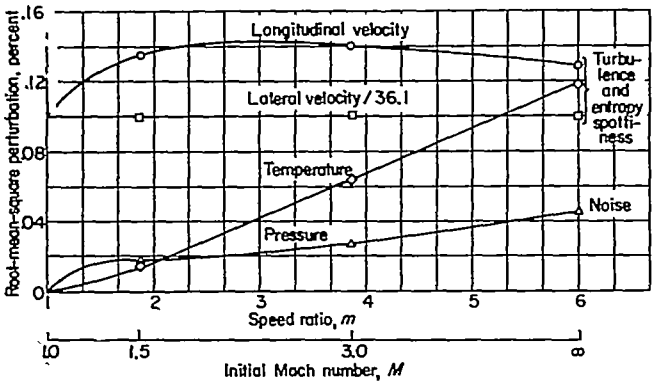

FIGURE 5.—Disturbances produced behind shock by interaction with strongly axisymmetric turbulence. Longitudinal intensity, 0.1 percent; lateral intensity is 3.61 percent just before shock. Root-mean-square velocity in percent of initial stream velocity; root-mean-square temperature and pressure in percent of ambient.

from above, approaching the limiting value of zero. The precise asymptotic expression is

$$0.1\sqrt{\frac{m\overline{p'^2}}{\overline{u^2}}}=0.1\frac{\gamma}{\gamma+1}\left(\frac{8}{5}\right)^{1/2}2^{1/4}(M-1)^{1/4} \tag{63}$$

where the omitted next-higher-order term is $0[(M-1)^{3/4}]$.

Figure 4 applies when isotropic turbulence flows into the shock. Figure 5 (prepared from calculations described in appendix B) applies when strongly axisymmetric turbulence flows into the shock; the specifications for the turbulence were taken from theoretical calculations of the modifications in initially isotropic turbulence that had passed through damping screens and a wind-tunnel contraction (ref. 10, four screens, $K=2$, $M=1.5$). The calculated deviation from isotropy is based on idealized conditions and is probably an extreme upper limit to what might be encountered in a wind-tunnel test section. The longitudinal component of the incident turbulence is the same for both figures—namely, 0.1 percent of free-stream speed—but the lateral component is 3.61 percent for figure 5 against 0.1 percent (isotropic) for figure 4. Despite the wide disparity in the lateral component, however, comparison of the two figures shows no great change in the curves. Evidently, the lateral component of the turbulence flowing into the shock has little effect, and the

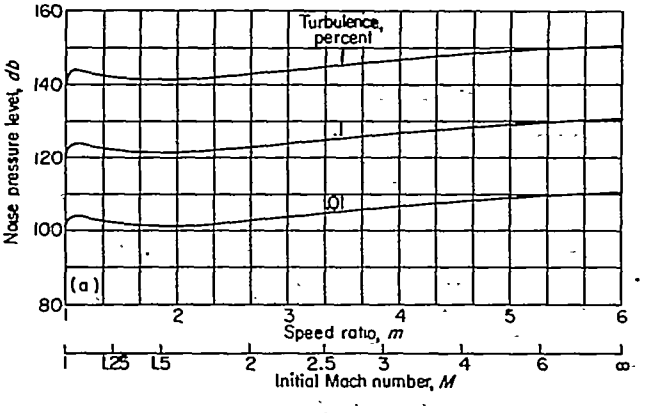

(a) Ambient pressure downstream of shock, 1 atmosphere.

FIGURE 6.—Noise generated by shock-turbulence interaction (isotropic turbulence).

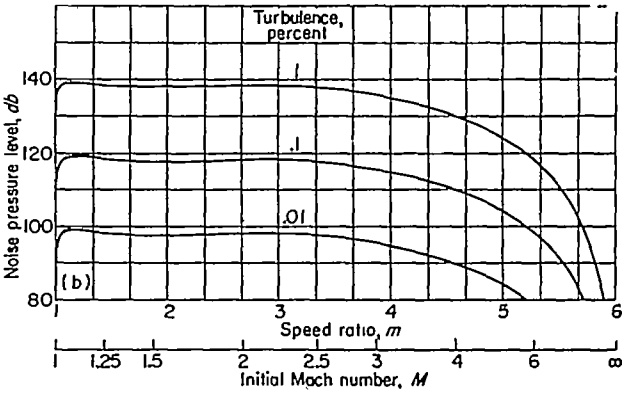

(b) Stagnation pressure upstream of shock, 1 atmosphere.

FIGURE 6.—Concluded. Noise generated by shock-turbulence interaction (isotropic turbulence).

intensity of the remainder of the disturbance field behind the shock depends almost solely on the longitudinal component, regardless of the degree of anisotropy. The shock-induced change in the lateral component itself, however, depends on the deviation from isotropy, being appreciable for the isotropic case and quite negligible for the extreme axisymmetric case.

The noise generated by the shock-turbulence interaction is measured by the curves of root-mean-square pressure. This is best indicated by use of an acoustic scale as in figure 6. Here the noise pressure level is plotted in decibels above the standard reference base of 0.000204 microbar for several levels of initial isotropic turbulence. According to the preceding paragraph there would be little difference for strongly axisymmetric turbulence of the same longitudinal intensities; the difference between figures 4 and 5 corresponds to no more than 4 decibels at the Mach numbers (1.5, 3, and ∞) for which there are comparable data.

The reference static pressure behind the shock is different for the two parts of figure 6. In figure 6(a) the ambient pressure behind the shock is constant with Mach number (1 atm): this situation may be approximated in an exit jet of an aircraft in flight. In figure 6(b) the stagnation pressure ahead of the shock is constant at 1 atmosphere, so that the static pressure behind the shock diminishes markedly with increasing Mach number; this situation is roughly characteristic of many wind-tunnel flows. It is seen that even at a longitudinal component of turbulence of 0.01 percent, the noise level is severe; and at 1 percent the noise level exceeds 130 decibels, which is of the order of the threshold of pain, over much of the Mach number range.

These remarks all refer to the asymptotic noise level an "infinite" distance behind the shock, since the attenuating part of the pressure waves has been neglected (in practice, this distance may be taken to be twice the longest significant wave length). For an initial Mach number of 1.5, the noise level is predicted to be some 17 decibels greater directly behind the shock where the attenuation is nil.

The local pressure level (proportional to the energy density) of the noise field in the region of shock-turbulence interaction is one aspect of the noise problem. Lighthill (ref. 3) has investigated another aspect, namely, the flux of acoustic energy radiated from the interaction region as a result of

the convection of any specified volume of turbulence through a weak plane shock segment ($1 \leq M \leq 1.3$); the turbulence need not be homogeneous. The two quantities, energy density and flux of energy, are not simply related unless the wave pattern is simple, for example, parallel plane waves or concentric spherical waves.

CONCLUDING REMARKS

The quantitative effects of the interaction of a convected homogeneous field of turbulence with an extended plane shock have been calculated, including the pressure level of the noise generated in the process. The assumed conditions are closely approximated in a supersonic wind tunnel or duct with a normal shock: the shock, together with its images in the walls (if the latter are nearly parallel), behaves substantially like an extended plane shock for the purposes of the analysis. The approximation is still quite good for plane oblique shocks for that portion of the incident turbulence whose eddies are small compared with the tunnel diameter (spectral wave length $\ll$ tunnel diam.), and probably fairly good even without this restriction on eddy size.

The propulsive free jet emitted by a turbojet, ram-jet, or rocket engine is turbulent, but the turbulence is far from homogeneous. In addition, only local segments of the shock structure that may occur aft of the nozzle can be considered sensibly plane. The shock-interaction noise generated by turbulent eddies smaller than such shock segments can perhaps be estimated from the curves presented herein. Estimates of this sort refer to the sound pressure level within the jet and nearby outside; they provide no direct information on the sound pressure level far from the jet as a function of distance and direction, or on the total acoustic power radiated by the jet.

Lewis Flight Propulsion Laboratory
National Advisory Committee for Aeronautics
Cleveland, Ohio, *June 3, 1954*

APPENDIX A

SYMBOLS

The following symbols are used in this report: (In appendix B some alternate symbols are defined and used in certain parts.)

a	function defined in ref. 2
a^*	critical speed of sound
b	function defined in ref. 2
$F(k)$	arbitrary function of k
$G(\Theta)$	screen-effect function, $G(\Theta)=\dfrac{4\alpha^2 \sin^2 \Theta+\nu^2 \cos^2 \Theta}{4 \sin^2 \Theta+\mu^2 \cos^2 \Theta}$
$H(\Theta)$	contraction-effect function, $H(\Theta)=\dfrac{l_2^2}{l_1}\dfrac{1}{(\epsilon \sin^2 \Theta+\cos^2 \Theta)^2}$
J'	Jacobian of transformation from k to $\underline{k}'$, $J'=\dfrac{d\underline{k}}{d\underline{k}'}=\dfrac{1}{m}$
J''	Jacobian of transformation from $\underline{k}$ to $\underline{k}''$, $J''=\dfrac{d\underline{k}}{d\underline{k}''}=\dfrac{\cos^2 \theta''}{m \cos^2 \theta'}\dfrac{\partial \theta'}{\partial \theta''}$
K	screen coefficient, $K=\dfrac{\text{pressure drop}}{\text{dynamic pressure}}$
k	amplitude of $\underline{k}$: $k^2=k_1^2+k_2^2+k_3^2=k_1^2+k_r$
k_r	radial component of $\underline{k}$, $k_r=-k_1 \cot \theta$
$\underline{k}$	wave-number vector, $\underline{k}=k_1, k_2, k_3$; also, $\underline{k}=k_1, k_r, 0$ in cylindrical coordinates
$d\underline{k}$	volume element in wave-number space, $d\underline{k}=dk_1dk_2dk_3$
l_1	contraction parameter, $l_1=\dfrac{\text{final stream speed}}{\text{initial stream speed}}$
l_2	contraction parameter, $l_2=\dfrac{\text{final stream-tube width}}{\text{initial stream-tube width}}$
M	Mach number upstream of normal shock
M_1	Mach number downstream of normal shock
m	ratio of speeds before and after shock, $m=\dfrac{(\gamma+1)M^2}{2+(\gamma-1)M^2}$
N	number of damping screens
P	transfer function for sound waves (pressure effect), $P=\dfrac{-2\gamma\sqrt{m}\Pi \sec \theta \sec \theta'}{(\gamma+1)m-(\gamma-1)}$
p	$\dfrac{\text{pressure perturbation}}{\text{mean static pressure}}$
$R_{ij}(\underline{\xi})$	perturbation velocity correlation tensor (special case of $\overline{\alpha\beta}(\underline{\xi})$)
r_{ij}	direction cosines
S	transfer function for shear waves, tabulated in tables I(c) to (k) (eq. in ref. 2)
T	$\dfrac{2(\gamma-1)(m-1)^2}{\sqrt{m}\,[(\gamma+1)m-(\gamma-1)]}\sqrt{(a \tan \theta-1)^2+(b \tan \theta)^2}$, $0 \leq \theta \leq \dfrac{\pi}{2}$
$\underset{\sim}{T}$	Transfer function for entropy waves (temperature effect) $\underset{\sim}{T}=Te^{i\delta}T$
U	stream velocity downstream of shock
U_A	stream velocity upstream of shock
u, v, w	nondimensional disturbance velocity components in directions x_1, x_2, x_3, respectively; $u, v, w=\dfrac{\text{components of velocity perturbation}}{\text{critical speed of sound } a^*}$
V	cross-stream velocity (sketch (c))
v_r	disturbance velocity component in radial direction/a^*
v_φ	disturbance velocity component in φ-direction/a^*
W	resultant of U and V
dW_β	(complex) wave amplitude in two-dimensional field

X transfer function, $X=Se^{i\delta_s}\dfrac{\cos\theta'}{\cos\theta}$

$\underline{x}$ position vector, $\underline{x}=x_i=x_1, x_2, x_3$

Y transfer function, $Y=Se^{i\delta_s}\dfrac{\sin\theta'}{\sin\theta}$

dZ_r (complex) wave amplitude associated with v_r

dZ_α (complex) wave amplitude associated with α

dZ_φ (complex) wave amplitude associated with v_φ

α, β may stand for u, v, w, p, ρ, or τ

α_s screen parameter, $\alpha_s^2=\dfrac{1.21}{1+K}$ for $K\geq 1$

$\overline{\alpha\beta}(\underline{\xi})$ correlation of α and β at a separation $\underline{\xi}$

$[\alpha\beta](\underline{k})$ Fourier transform of $\overline{\alpha\beta}(\underline{\xi})$, interpreted as spectral density of $\overline{\alpha\beta}(0)$

β_w $\sqrt{\dfrac{M_1^2}{\cos^2\theta'}}-1$

$\Gamma_{ij}(\underline{k})$ perturbation velocity spectrum tensor (special case of $[\alpha\beta]\underline{k}$)

γ ratio of specific heats (taken as 1.4)

δ_p phase angle of $\underset{\sim}{\Pi}$ (eq. in ref. 2)

δ_s phase angle of X and Y, tabulated in tables I(c) to (k) (eq. in ref. 2)

δ_T phase angle of $\underset{\sim}{T}$, tabulated in tables I(c) to (k), $\delta_T=\tan^{-1}\left(\dfrac{b}{\cot\theta-a}\right)$, $0\leq\theta\leq\dfrac{\pi}{2}$

ϵ contraction parameter, $\epsilon=l_2^2/l_1^2$

Θ shear-wave inclination ahead of contraction, $\Theta=\tan^{-1}\left(\dfrac{l_1}{l_2}\tan\theta\right)$

θ shear-wave inclination ahead of shock (see fig. 3)

θ' shear-wave inclination behind shock (see fig. 3), $\theta'=\tan^{-1}(m\tan\theta)$

θ'' sound-wave inclination behind shock (see fig. 3),

$$\theta''=\begin{cases}-\tan^{-1}\dfrac{M^2\tan\theta}{1-M^2}, & 0\leq\theta\leq\theta_{cr}\\ \theta'-\cot^{-1}\beta_w, & \theta_{cr}\leq\theta\leq\dfrac{\pi}{2}\end{cases}$$

θ_{cr} critical value of θ for which W=speed of sound

$\underline{\kappa}$ wave-number vector, $\underline{\kappa}=\kappa_1, \kappa_2, \kappa_3$

μ screen parameter, $\mu=1+\alpha_s+K$

ν screen parameter, $\nu=1+\alpha_s-\alpha_s K$

$\underline{\xi}$ separation of two points, $\underline{\xi}=\underline{\hat{x}}-\underline{x}$

Π function tabulated in table I (defined in ref. 2)

$\underset{\sim}{\Pi}$ transfer function for sound waves, $\underset{\sim}{\Pi}=\Pi e^{i\delta_p}$

ρ $\dfrac{\text{density perturbation}}{\text{mean density}}$

τ $\dfrac{\text{temperature perturbation}}{\text{mean temperature}}$

$\Phi_{ij}(\underline{k})$ perturbation velocity spectrum tensor (special case of $[\alpha\beta](\underline{k})$)

φ common longitude angle of wave normals $\underline{\kappa}$, $\underline{k}$, $\underline{k}'$, $\underline{k}''$ in polar coordinates

χ transfer function, $\chi=\underset{\sim}{\Pi}\dfrac{(\cos\theta'-e^{-in\pi/2}\beta_w\sin\theta')}{\cos\theta}$

Υ transfer function, $\Upsilon=\underset{\sim}{\Pi}\dfrac{(\sin\theta'+e^{in\pi/2}\beta_w\cos\theta')}{\sin\theta}$

where

$$n=1,\ 0\leq\theta\leq\theta_{cr}$$
$$=0,\ \theta_{cr}\leq\theta\leq\frac{\pi}{2}$$

ψ acute angle between oblique shock and upstream flow direction

Subscripts:

α, β may stand for u, v, w, p, ρ, or τ

i, j, m, n may stand for 1, 2, or 3; used to replace α and β when u, v, w are replaced by u_1, u_2, u_3, respectively

Superscripts:

$*$ complex conjugate

$'$ refracted shear-entropy wave

$''$ sound wave

$\wedge$ distinguishing mark

APPENDIX B

COMPLETE VELOCITY SPECTRUM TENSORS

The first and the sum of the second and third diagonal terms of the spectrum tensors of the velocity field behind the shock are obtained in the text by use of a simplified approach. Other terms are occasionally of interest; for example, the separate values of the second and third diagonal terms are needed for a description of anisotropic turbulence. The complete spectrum tensor for each field (turbulence and noise) will be derived herein by a more comprehensive procedure.

Turbulence field.—It will be convenient to replace the symbols u, v, w by u_1, u_2, u_3, and to replace α and β by i, j, which take on the values 1, 2, and 3 instead of u, v, and w. With this notation and the use of equations (8), equations (10) can be transformed to

$$dZ_1'=X\,dZ_1$$
$$dZ_2'=(Y-1)dZ_r\cos\varphi+dZ_2$$
$$dZ_3'=(Y-1)dZ_r\sin\varphi+dZ_3$$

By introduction of the geometric relations (figs. 1 and 2)

$$\left.\begin{aligned}dZ_r&=dZ_1\tan\theta\\ \tan\theta&=-k_1/k_r\\ \cos\varphi&=-k_2/k_r\\ \sin\varphi&=-k_3/k_r\end{aligned}\right\}\qquad\text{(B1)}$$

all three equations may be represented by the single expression

$$dZ_i'=X\,dZ_1\delta_{1i}+\left[(Y-1)\left(-\frac{k_1k_\alpha}{k_r^2}\right)dZ_1+dZ_i\right](1-\delta_{1i})\qquad\text{(B2)}$$

where

$$\delta_{1i}=\begin{Bmatrix}1, & i=1\\ 0, & i\neq 1\end{Bmatrix}$$

Multiplication of the complex conjugate of equation (B2) by the corresponding equation with subscript j and by k_r^4 yields, after averaging,

$$\begin{aligned}k_r^4\overline{dZ_i'^*dZ_j'}=&k_r^4|X|^2\overline{|dZ_1|^2}\delta_{1i}\delta_{1j}+(1-\delta_{1i})(1-\delta_{1j})\times\\&[k_1^2k_ik_j|Y-1|^2\overline{|dZ_1|^2}+k_r^4\overline{dZ_i^*dZ_j}+\\&k_1k_ik_r^2(1-Y^*)\overline{dZ_1^*dZ_j}+k_ik_jk_r^2(1-Y)\overline{dZ_1dZ_i^*}]+\\&\delta_{1i}(1-\delta_{1j})X^*[k_1k_jk_r^2(1-Y)\overline{|dZ_1|^2}+k_r^4\overline{dZ_i^*dZ_j}]+\\&\delta_{1j}(1-\delta_{1i})X[k_1k_ik_r^2(1-Y^*)\overline{|dZ_1|^2}+k_r^4\overline{dZ_1dZ_i^*}]\end{aligned}\quad\text{(B3)}$$

Now, if in equation (15) the symbol for the spectral tensor is changed from $\alpha\beta$ to the more conventional symbol Φ_{ij}, application to equation (B3) yields

$$\begin{aligned}\Phi_{ij}'d\underline{k}'=\Bigg\{&\frac{d\underline{k}}{k_r^4}k_r^4|X|^2\Phi_{11}\delta_{1i}\delta_{1j}+(1-\delta_{1i})(1-\delta_{1j})[k_1^2k_ik_j|Y-1|^2\Phi_{11}+\\&k_r^4\Phi_{ij}+k_1k_ik_r^2(1-Y^*)\Phi_{1j}+k_1k_jk_r^2(1-Y)\Phi_{1i}^*]+\\&\delta_{1i}(1-\delta_{1j})X^*[k_1k_jk_r^2(1-Y)\Phi_{11}+k_r^4\Phi_{1j}]+\\&\delta_{1j}(1-\delta_{1i})X[k_1k_ik_r^2(1-Y^*)\Phi_{11}+k_r^4\Phi_{1i}]\Bigg\}\end{aligned}\quad\text{(B4)}$$

The elements of the turbulence spectrum tensor Φ_{ij} may be exhibited in expanded matrix form:

$$\Phi_{ij}'d\underline{k}'=\frac{d\underline{k}}{k_r^4}\begin{array}{|c|c|c|}\hline k_r^4|X|^2\Phi_{11} & X^*[k_1k_2k_r^2(1-Y)\Phi_{11}+k_r^4\Phi_{12}] & X^*[k_1k_3k_r^2(1-Y)\Phi_{11}+k_r^4\Phi_{13}]\\\hline & k_r^4\Phi_{22}+k_1^2k_2^2|Y-1|^2\Phi_{11}+k_1k_2k_r^2(1-Y^*)\Phi_{12}+k_1k_2k_r^2(1-Y)\Phi_{12}^* & k_r^4\Phi_{23}+k_1^2k_2k_3|Y-1|^2\Phi_{11}+k_1k_2k_r^2(1-Y^*)\Phi_{13}+k_1k_3k_r^2(1-Y)\Phi_{12}^*\\\hline & & k_r^4\Phi_{33}+k_1^2k_3^2|Y-1|^2\Phi_{11}+k_1k_3k_r^2(1-Y^*)\Phi_{13}+k_1k_3k_r^2(1-Y)\Phi_{13}^*\\\hline\end{array}$$

The matrix is Hermitian; that is, the missing elements are the complex conjugates of the respective elements diagonally opposite; that is, $\Phi_{21}^{*\prime}=\Phi_{12}'$, and so forth.

It can be shown, by use of the continuity relation $k_i\Phi_{ij}=k_j\Phi_{ij}=0$ (summed over repeated index), that after some reduction

$$(\Phi_{22}'+\Phi_{33}')\,d\underline{k}'=\left[(|Y|^2-1)\,\Phi_{11}\frac{k_1^2}{k_r^2}+\Phi_{22}+\Phi_{33}\right]d\underline{k}$$

in agreement with the second of equations (29).

Noise field.—With use of equations (B1), the three equations (11) may be represented by the single expression

$$dZ_i''=\chi\,dZ_1\delta_{1i}-\Upsilon\left(\frac{k_1k_\alpha}{k_r^2}\right)dZ_1\,(1-\delta_{1i})\quad\text{(B5)}$$

where again the subscripts 1, 2, 3 replace u, v, w, and $\delta_{1i}=0$ or 1 as before. Starting with this equation, the spectral tensor Φ_{ij}'' may be derived in a straightforward manner by a procedure parallel to that leading from equation (B2) to (B4). The result is

$$\begin{aligned}\Phi_{ij}''\,d\underline{k}''=\Phi_{11}\,d\underline{k}\Bigg\{&|\chi|^2\,\delta_{1i}\delta_{1j}+|\Upsilon|^2\frac{k_1^2k_ik_j}{k_r^4}(1-\delta_{1i})(1-\delta_{1j})-\\&\frac{k_1}{k_r^2}|\chi||\Upsilon|[\delta_{1i}(1-\delta_{1j})k_j+\delta_{1j}(1-\delta_{1i})k_i]\Bigg\}\end{aligned}\quad\text{(B6)}$$

(The valid range of this equation has been limited to $\theta_{cr}\leq|\theta|\leq\frac{\pi}{2}\left(\left|\frac{k_1}{k_r}\right|\geq\tan\theta_{cr}\right)$ by use of the simplification $\chi\Upsilon^*=\chi^*\Upsilon=|\chi||\Upsilon|$, which fails outside that range.)

The expanded form of equation (B6) is

$$\Phi_{ij}''d\underline{k}''=\Phi_{11}\frac{d\underline{k}}{k_r^4}\begin{vmatrix}|\chi|^2k_r^4 & -|\chi||\Upsilon|k_1k_2k_r^2 & -|\chi||\Upsilon|k_1k_3k_r^2\\-|\chi||\Upsilon|k_1k_2k_r^2 & |\Upsilon|^2k_1^2k_2^2 & -|\Upsilon|^2k_1^2k_2k_3\\-|\chi||\Upsilon|k_1k_3k_r^2 & -|\Upsilon|^2k_1^2k_2k_3 & |\Upsilon|^2k_1^2k_3^2\end{vmatrix}$$

The diagonal terms yield

$$\Phi_{11}''d\underline{k}''=|\chi|^2\Phi_{11}\,d\underline{k}$$

$$(\Phi_{22}''+\Phi_{33}'')d\underline{k}''=|\Upsilon|^2\frac{k_1^2}{k_r^2}\Phi_{11}\,d\underline{k}$$

since $k_2^2+k^2=k_r^2$; these are in agreement with equations (30).

APPENDIX C

CALCULATIONS FOR AXISYMMETRIC INITIAL TURBULENCE

If the turbulence in the settling chamber of a supersonic wind tunnel is considered to be isotropic, by the time it reaches the working section it will be axisymmetric, with the longitudinal velocity perturbations very much less than the lateral perturbations; the change is due to the effects of the damping screens and the contraction (refs. 9, 13, and 14). The shock-interaction behavior for a particular case of extreme axisymmetry will be calculated herein as a matter of interest.

According to reference 14 (with a slight change in notation), if the longitudinal spectral density in the settling chamber (station A′) is written as

$$[uu]_0=\kappa^2F(\kappa)\cos^2\Theta\quad\text{(isotropic turbulence)}$$

then the longitudinal density in the working section (station A) is given by

$$[uu]=\kappa^2F(\kappa)\cos^2\Theta G^N(\Theta)H(\Theta)\quad\text{(axisymmetric turbulence)}\quad\text{(C1)}$$

where κ is the wave number at A', Θ is the associated wave inclination, N is the number of damping screens, $G(\Theta)$ depends on the screen pressure-drop coefficient K, and $H(\Theta)$ depends on the parameters l_1 and l_2 defining the wind-tunnel

contraction. (See appendix A for the functional forms.) In what follows, $N=4$, $K=2$, $l_1=24.92$, and $l_2=0.3186$.[7] This set of values corresponds (in theory) to an axisymmetric turbulence at station A (just upstream of the shock) such that the root-mean-square lateral velocity component is 36.1 times the root-mean-square longitudinal component (see table I, p. 46, ref. 14). The ratio 36.1:1 is clearly an extreme deviation from isotropy.

The effects of the changed form of $[uu]$ on the integration procedure will be illustrated by considering the mean-square longitudinal velocity in the turbulence. The relevant question is (53), with $[uu]$ being given by equation (C1). From the form of equation (C1) it will be convenient to carry out the integrations in terms of $\underline{\kappa}$, rather than $\underline{k}$; the transformation is

$$d\underline{k}=\frac{1}{l_1 l_2^2}\,d\underline{\kappa}=\frac{1}{l_1 l_2^2}\,\kappa^2 d\kappa d\varphi \cos\Theta\, d\Theta$$

Equation (35) then assumes the form

$$\overline{u'^2}=\frac{2}{l_1 l_2^2}\int_0^{\pi/2}|S|^2\frac{\cos^2\theta'}{\cos^2\theta}\,G^N H\cos^3\Theta\, d\Theta\int_0^{\infty}\kappa^4 G(\kappa)\,d\kappa\int_0^{2\pi}d\varphi$$

The last two integrals appear in the expression for $\overline{u_0^2}$, the mean-square longitudinal velocity at station A' (the expression is of the form of eq. (57)); thus, equation (C2) may be simplified to

$$\frac{\overline{u'^2}}{\overline{u_0^2}}=\left(\frac{3/2}{l_1 l_2^2}\right)\int_0^{\pi/2}|S|^2\frac{\cos^2\theta'}{\cos^2\theta}\,G^N H\cos^3\Theta\, d\Theta \qquad \text{(C3)}$$

The variable of integration may be changed from Θ to θ by means of the transformation

$$d\Theta=\frac{1}{\sqrt{\epsilon}}\frac{\cos^2\Theta}{\cos^2\theta}\,d\theta$$

This results in the alternate form

$$\frac{\overline{u'^2}}{\overline{u_0^2}}=\left(\frac{3/2}{l_1 l_2^2}\right)\int_0^{\pi/2}|S|^2\frac{\cos^2\theta'}{\cos^2\theta}\,G^N H\frac{\cos^2\Theta}{\cos^2\theta}\frac{\cos^3\Theta\, d\Theta}{\sqrt{\epsilon}} \qquad \text{(C4)}$$

On numerical evaluation, the integrand of equation (C3) was found to have a sharp peak near the upper limit, and that of (C4) a sharp peak at the origin. The peaks were avoided by dividing the range of numerical integration among the two equations: (C3) was used over the range $0<\Theta<\Theta_1$ and (C4) was used over the range $5°<\theta<90°$, where Θ_1 is the value of Θ corresponding to $\theta=5°$.

REFERENCES

1. Lighthill, M. J.: On Sound Generated Aerodynamically. I—General Theory. Proc. Roy. Soc. (London), ser. A, vol. 211, no. 1107, Mar. 20, 1952, pp. 564–587.
2. Ribner, H. S.: Convection of a Pattern of Vorticity Through a Shock Wave. NACA Rep. 1164, 1954. (Supersedes NACA TN 2864.)
3. Lighthill, M. J.: On the Energy Scattered from the Interaction of Turbulence with Sound or Shock Waves. Proc. Cambridge Phil. Soc., vol. 49, pt. 3, July 1953, pp. 531–551.
4. Moore, Franklin K.: Unsteady Oblique Interaction of a Shock Wave with a Plane Disturbance. NACA Rep. 1165, 1954. (Supersedes NACA TN 2879.)
5. Kovásznay, Leslie S. G.: Turbulence in Supersonic Flow. Jour. Aero. Sci., vol. 20, no. 10, Oct. 1953, pp. 657–674; 682.
6. Chang, C. T.: On the Interaction Between Weak Fluctuating Fields of Sound, Vorticity, and Temperature with an Oscillating Shock. Pt. I—In an Infinitely Extended Medium. Dept. Aero., The Johns Hopkins Univ., Dec. 1, 1953. (Contract N6ori-105, Task Order III.)
7. Moore, Franklin K.: Passage of Flow Disturbances Through a Duct Containing Screens, Shocks, or Contractions. Proc. Third Midwestern Conf. on Fluid Mech., Univ. of Minn., 1953, pp. 193–216.
8. Ribner, H. S., and Moore, F. K.: Unsteady Interaction of Disturbances with a Shock Wave, with Applications to Turbulence and Noise. Heat Transfer and Fluid Mech. Inst., Stanford Univ. Press, 1953, pp. 45–55.
9. Ribner, H. S., and Tucker, M.: Spectrum of Turbulence in a Contracting Stream. NACA Rep. 1113, 1953. (Supersedes NACA TN 2606.)
10. Moyal, J. E.: The Spectra of Turbulence in a Compressible Fluid; Eddy Turbulence and Random Noise. Proc. Cambridge Phil. Soc., vol. 48, pt. 2, Apr. 1952, pp. 329–344.
11. James, Hubert M., Nickols, Nathaniel B., and Phillips, Ralph S., eds.: Theory of Servomechanisms. First ed., McGraw-Hill Book Co., Inc., 1947, pp. 262–308.
12. Batchelor, G. K.: The Theory of Homogeneous Turbulence. Cambridge Univ. Press, 1953.
13. Taylor, G. I., and Batchelor, G. K.: The Effect of Wire Gauze on Small Disturbances in a Uniform Stream. Quart. Jour. Mech. Appl. Math., vol. II, 1949, pp. 1–29.
14. Tucker, Maurice: Combined Effect of Damping Screens and Stream Convergence on Turbulence. NACA TN 2878, 1953.

[7] The values of l_1 and l_2 correspond to Mach numbers of 0.05 and 1.5 at stations A' and A, respectively. In the calculations, however, these same values of l_1 and l_2 will be maintained even though the Mach number at A is varied, in order to maintain the turbulent spectrum unchanged.

TABLE I.—WAVE ANGLES AND TRANSFER FUNCTIONS

(a) $M=1.01$ ($m=1.01669$) (abbreviated table)

θ, deg	θ', deg	θ'', deg	Π
7.92542(θ_{cr})	8.056	−81.944	1.6345
7.95000	8.081	−81.281	1.3923
7.97500	8.106	−80.988	1.3017
8.00000	8.132	−80.757	1.2363
8.25000	8.386	−79.278	.9132
8.43785	8.577	−78.471	.7870
8.95028	9.097	−76.662	.5826
9.46271	9.618	−75.111	.4633
9.97514	10.138	−73.686	.3824
10.48757	10.659	−72.339	.3232
11.0	11.179	−71.045	.2778
12.5	12.702	−67.445	.1902
14	14.224	−64.014	.1383
15	15.239	−61.783	.1142
20	20.307	−50.990	.0508
25	25.365	−40.502	.0251
30	30.412	−30.164	.0124
35	35.447	−19.916	.0057
40	40.468	−9.739	.0019
45	45.474	.384	−.0001
50	50.466	10.460	−.0011
55	55.444	20.495	−.0014
60	60.409	30.493	−.0014
65	65.361	40.461	−.0012
70	70.303	50.401	−.0008
75	75.235	60.320	−.0005
80	80.161	70.223	−.0002
85	85.082	80.114	−.0001
90	90	90	--------

(b) $M=1.05$ ($m=1.08398$) (abbreviated table)

θ, deg	θ', deg	θ'', deg	Π
16.323(θ_{cr})	17.61	−72.39	1.5246
16.400	17.69	−70.59	1.2371
16.630	17.94	−68.59	.9995
16.936	18.27	−66.81	.8375
17.240	18.59	−65.35	.7307
17.549	18.92	−64.05	.6499
18.162	19.58	−61.74	.5336
18.775	20.23	−59.66	.4508
19.388	20.88	−57.72	.3876
20.001	21.53	−55.88	.3377
25	26.82	−42.64	.1357
30	32.04	−30.75	.0611
35	37.20	−19.49	.0257
40	42.29	−8.62	.0076
45	47.31	1.96	−.0016
50	52.26	12.30	−.0058
55	57.14	22.44	−.0071
60	61.96	32.41	−.0067
65	66.72	42.23	−.0055
70	71.44	51.93	−.0039
75	76.12	61.53	−.0024
80	80.76	71.06	−.0011
85	85.39	80.54	−.0003
90	90	90	--------

(c) $M=1.10$ ($m=1.16908$)

θ, deg	θ', deg	θ'', deg	S	Π	T	δ_s, deg	δr, deg
0	0	0	1.145	[a]1.6667	−0.008792	0	180.00
5	5.84	−26.75	1.145	[a]1.6508	−.008788	.49	156.00
10	11.65	−45.45	1.148	[a]1.6048	−.008777	.90	129.76
15	17.39	−57.07	1.152	[a]1.5318	−.008767	1.11	97.30
18	20.80	−61.89	1.157	[a]1.4779	−.008770	1.01	70.12
20	23.05	−64.51	1.161	[a]1.4392	−.008780	.70	41.90
20.268	23.35	−64.83	1.161	[a]1.4339	−.008783	.62	36.37
20.536	23.65	−65.14	1.162	[a]1.4286	−.008786	.51	29.73
20.804	23.95	−65.45	1.162	[a]1.4233	−.008789	.37	21.07
21.072(θ_{cr})	24.25	−65.75	1.163	1.4179	−.008791	0	0
21.100	24.28	−64.45	1.161	1.2582	−.007808		
21.400	24.62	−61.02	1.155	.9378	−.005845		
21.800	25.06	−58.41	1.152	.7620	−.004779		
22.200	25.50	−56.34	1.149	.6511	−.004111		
22.560	25.90	−54.69	1.147	.5769	−.003663		
24.048	27.55	−48.95	1.141	.3356	−.002511		
25.536	29.18	−44.07	1.135	.2778	−.001860		
27.024	30.81	−39.59	1.130	.2066	−.001428		
28.512	32.42	−35.38	1.125	.1561	−.001037		
30	34.02	−31.36	1.121	.1187	−.000873		
35	39.30	−18.76	1.105	.0448	−.000373		
40	44.45	−7.08	1.090	.0105	−.000101		
45	49.46	3.98	1.075	−.0057	−.000066		
50	54.33	14.68	1.060	−.0125	−.000176		
55	59.08	24.78	1.047	−.0141	−.000252		
60	63.72	34.66	1.035	−.0129	−.000307		
65	68.26	44.28	1.025	−.0103	−.000346		
70	72.71	53.68	1.016	−.0072	−.000374		
75	77.09	62.91	1.009	−.0043	−.000395		
80	81.42	72.01	1.004	−.0020	−.000408		
85	85.72	81.02	1.001	−.0005	−.000416		
90	90	90	-----	0	---------		

(d) $M=1.25$ ($m=1.42857$)

θ, deg	θ', deg	θ'', deg	S	Π	T	δ_s, deg	δr, deg
0	0	0	1.300	[a]1.6667	−0.04059	0	180.00
5	7.12	−13.66	1.302	[a]1.6453	−.04054	1.57	163.64
10	14.14	−26.09	1.307	[a]1.5840	−.04040	2.98	146.17
15	20.95	−36.66	1.317	[a]1.4882	−.04018	4.04	125.99
20	27.47	−45.31	1.335	[a]1.3684	−.03998	4.47	99.05
23	31.23	−49.70	1.353	[a]1.2926	−.04009	4.11	76.76
25	33.67	−52.33	1.371	[a]1.2466	−.04019	3.22	53.40
26	34.87	−53.57	1.383	[a]1.2229	−.04039	2.20	34.30
26.300	35.22	−53.93	1.387	[a]1.2172	−.04048	1.67	25.44
26.656(θ_{cr})	35.65	−54.35	1.392	1.2106	−.04059	0	0
26.742	35.75	−51.36	1.373	.969	−.03261		
26.828	35.85	−50.07	1.366	.884	−.02980		
26.914	35.95	−49.05	1.360	.822	−.02774		
27	36.05	−48.15	1.356	.773	−.02613		
27.5	36.64	−44.27	1.338	.593	−.02029		
28	37.22	−41.28	1.326	.484	−.01680		
29	38.38	−36.35	1.307	.3484	−.01237		
30	39.52	−32.16	1.293	.2614	−.00953		
35	45.01	−15.45	1.238	.0658	−.00276		
40	50.16	−1.86	1.195	−.0007	−.00004		
45	55.01	10.13	1.157	−.0261	−.00157		
50	59.57	21.02	1.123	−.0337	−.00252		
55	63.89	31.10	1.094	−.0327	−.00316		
60	67.99	40.54	1.068	−.0277	−.00360		
65	71.92	49.48	1.047	−.0211	−.00392		
70	75.71	58.02	1.030	−.0143	−.00414		
75	79.38	66.27	1.017	−.0084	−.00430		
80	82.96	74.29	1.008	−.0038	−.00440		
85	86.50	82.18	1.002	−.0010	−.00446		
90	90	90	-----	--------	---------		

[a] These values apply for $x=0$ only. For $x=\infty$, values should be replaced by 0. All other values are independent of x.

TABLE I.—WAVE ANGLES AND TRANSFER FUNCTIONS—Continued

(e) $M=1.5$ ($m=1.86207$)

θ, deg	θ', deg	θ'', deg	S	Π	T	δ_s, deg	δ_T, deg
0	0	0	1.463	*1.6667	−0.1071	0	180.00
5	9.25	−8.95	1.466	*1.6346	−.1068	3.43	167.04
10	18.18	−17.61	1.476	*1.5441	−.1060	6.48	153.24
15	26.52	−25.75	1.494	*1.4085	−.1047	8.79	137.43
20	34.13	−33.23	1.527	*1.2464	−.1030	10.01	117.24
25	40.97	−40.01	1.594	*1.0850	−.1019	9.34	85.17
27	43.49	−42.52	1.649	*1.0366	−.1030	7.60	61.42
28	44.71	−43.74	1.693	*1.0249	−.1050	5.38	40.29
28.300	45.07	−44.10	1.710	*1.0240	−.1058	4.10	29.96
28.644(θ_{cr})	45.49	−44.51	1.733	1.0254	−.1071	0	0
28.670	45.52	−42.58	1.699	.8849	−.0925	↓	↓
28.733	45.59	−40.93	1.674	.7831	−.0820		
28.750	45.61	−40.60	1.668	.7634	−.0800		
28.822	45.70	−39.36	1.652	.6973	−.0733		
28.911	45.80	−38.10	1.636	.6382	−.0671		
29.0	45.91	−37.06	1.623	.5913	−.0624		
29.5	46.49	−32.62	1.576	.429	−.0460		
30	47.07	−29.21	1.544	.332	−.0362		
30.5	47.64	−26.31	1.520	.266	−.0294		
31.0	48.21	−23.69	1.499	.214	−.0241		
31.5	48.77	−21.30	1.481	.174	−.0199		
32	49.32	−19.06	1.465	.141	−.0164		
33	50.41	−14.96	1.437	.0905	−.0109		
34	51.47	−11.21	1.412	.0536	−.0067		
35	52.51	−7.73	1.390	.0258	−.0033		
36	53.53	−4.45	1.369	.0042	−.0005		
37	54.52	−1.35	1.350	−.0123	−.0017		
38	55.50	1.60	1.332	−.0254	−.0037		
39	56.45	4.42	1.316	−.0356	−.0054		
40	57.38	7.13	1.300	−.0435	−.0068		
45	61.76	19.32	1.231	−.0618	−.0119		
50	65.74	29.87	1.176	−.0613	−.0149		
55	69.39	39.25	1.130	−.0531	−.0169		
60	72.77	47.78	1.093	−.0421	−.0183		
65	75.94	55.67	1.063	−.0307	−.0192		
70	78.94	63.06	1.040	−.0203	−.0199		
75	81.81	70.09	1.022	−.0117	−.0204		
80	84.59	76.86	1.010	−.0053	−.0207		
85	87.31	83.47	1.002	−.0013	−.0209		
90	90	90	-----	-------	---------	↓	↓

(f) $M=2.0$ ($m=2.66667$)

θ, deg	θ' deg	θ'', deg	S	Π	T	δ_s, deg	δ_T, deg
0	0	0	1.625	*1.6667	−0.2268	0	180.00
5	13.13	−6.65	1.631	*1.6094	−.2258	6.76	168.99
10	25.18	−13.23	1.649	*1.4571	−.2225	12.35	157.21
15	35.55	−19.66	1.683	*1.2507	−.2166	16.03	143.52
20	44.14	−25.89	1.744	*1.0266	−.2072	17.43	125.51
25	51.19	−31.87	1.879	*.8205	−.1966	15.80	93.97
26	52.44	−33.04	1.939	*.7933	−.1970	14.68	82.19
27	53.65	−34.19	2.042	*.7873	−.2029	12.45	63.44
27.5	54.23	−34.76	2.134	*.8051	−.2113	9.87	46.63
27.938(θ_{cr})	54.74	−35.26	2.274	.8503	−.2268	0	0
27.960	54.76	−33.26	2.179	.7007	−.1870	↓	↓
27.988	54.79	−32.16	2.137	.6332	−.1691		
28.038	54.85	−30.84	2.090	.5614	−.1503		
28.138	54.96	−28.99	2.033	.4745	−.1275		
28.238	55.07	−27.51	1.992	.4146	−.1119		
28.338	55.19	−26.24	1.960	.3692	−.1000		
28.5	55.37	−24.47	1.920	.3123	−.0851		
29	55.92	−20.13	1.834	.2013	−.0559		
30	57.00	−13.65	1.731	.0855	−.0247		
32	59.03	−4.00	1.606	−.0190	−.0059		
35	61.83	6.97	1.487	−.0795	−.0280		
40	65.92	20.95	1.355	−.1047	−.0456		
45	69.44	31.99	1.262	−.0996	−.0546		
50	72.53	41.21	1.192	−.0851	−.0600		
55	75.29	49.19	1.138	−.0680	−.0636		
60	77.78	56.28	1.096	−.0513	−.0660		
65	80.08	62.72	1.064	−.0362	−.0677		
70	82.23	68.68	1.040	−.0234	−.0689		
75	84.26	74.29	1.022	−.0133	−.0698		
80	86.22	79.66	1.010	−.0059	−.0703		
85	88.12	84.86	1.002	−.0015	−.0706		
90	90	90	-----	-------	---------	↓	↓

(g) $M=2.5$ ($m=3.33333$)

θ, deg	θ', deg	θ'', deg	S	Π	T	δ_s, deg	δ_T, deg
0	0	0	1.700	*1.6667	−0.3139	0	180.00
5	16.26	−5.95	1.708	*1.5839	−.3119	9.39	169.66
10	30.44	−11.86	1.734	*1.3774	−.3055	16.57	158.51
15	41.77	−17.69	1.783	*1.1220	−.2933	20.54	145.33
20	50.50	−23.43	1.869	*.8638	−.2722	21.12	127.29
20.832	51.75	−24.37	1.890	*.8219	−.2675	20.86	123.33
21.664	52.94	−25.31	1.913	*.7807	−.2625	20.50	118.87
22.496	54.08	−26.24	1.941	*.7404	−.2573	20.00	113.76
23.328	55.18	−27.18	1.976	*.7014	−.2519	19.36	107.69
24.160	56.23	−28.10	2.021	*.6657	−.2472	18.53	100.16
24.992	57.24	−29.03	2.086	*.6375	−.2448	17.42	89.96
25.824	58.20	−29.95	2.209	*.6323	−.2511	15.60	73.46
26.656(θ_{cr})	59.14	−30.86	2.662	.7638	−.3139	0	0
26.675	59.16	−28.86	2.496	.5957	−.2448	↓	↓
26.706	59.19	−27.57	2.413	.5120	−.2108		
26.756	59.25	−26.18	2.337	.4366	−.1801		
26.856	59.36	−24.16	2.244	.3470	−.1437		
26.956	59.46	−22.61	2.184	.2898	−.1206		
27.056	59.57	−21.27	2.138	.2469	−.1032		
27.492	60.04	−16.76	2.008	.1337	−.0568		
27.792	60.35	−14.29	1.949	.0866	−.0373		
28.328	60.90	−10.52	1.870	.0290	−.0128		
28.528	61.11	−9.26	1.846	.0129	−.0057		
28.750	61.33	−7.94	1.822	−.0026	−.0012		
29.164	61.74	−5.63	1.781	−.0266	−.0121		
29.264	61.84	−5.10	1.772	−.0316	−.0144		
30	62.54	−1.46	1.715	−.0614	−.0290		
35	66.81	16.66	1.476	−.1288	−.0752		
40	70.33	29.31	1.340	−.1276	−.0932		
45	73.30	39.24	1.246	−.1109	−.1028		
50	75.87	47.46	1.177	−.0906	−.1087		
55	78.14	54.51	1.126	−.0705	−.1126		
60	80.17	60.74	1.087	−.0522	−.1153		
65	82.04	66.37	1.057	−.0364	−.1172		
70	83.77	71.55	1.035	−.0234	−.1186		
75	85.40	76.42	1.019	−.0132	−.1195		
80	86.97	81.06	1.008	−.0059	−.1201		
85	88.50	85.57	1.002	−.0015	−.1205		
90	90	90	-----	-------	---------	↓	↓

(h) $M=3.0$ ($m=3.85714$)

θ, deg	θ', deg	θ'', deg	S	Π	T	δ_s, deg	δ_T, deg
0	0	0	1.741	*1.6667	−0.3754	0	180.00
5	18.65	−5.62	1.751	*1.5610	−.3725	11.37	169.97
10	34.22	−11.22	1.784	*1.3125	−.3631	19.48	159.10
15	45.94	−16.78	1.845	*1.0270	−.3444	23.25	146.05
20	54.54	−22.27	1.953	*.7497	−.3098	22.74	127.56
23	58.58	−25.52	2.072	*.5894	−.2767	20.03	108.50
24	59.79	−26.60	2.144	*.5423	−.2658	18.56	97.65
25	60.93	−27.68	2.307	*.5271	−.2696	16.46	77.55
25.3	61.26	−28.00	2.437	*.5540	−.2871	15.13	64.65
25.644(θ_{cr})	61.63	−28.37	2.940	.7137	−.3754	0	0
25.650	61.64	−27.22	2.785	.5922	−.3114	↓	↓
25.670	61.66	−25.91	2.650	.4872	−.2564		
25.700	61.69	−24.74	2.553	.4118	−.2170		
25.744	61.74	−23.48	2.467	.3456	−.1825		
25.844	61.84	−21.41	2.351	.2586	−.1371		
25.944	61.95	−19.78	2.276	.2040	−.1086		
26.044	62.05	−18.44	2.221	.1649	−.0882		
26.250	62.27	−16.04	2.137	.1072	−.0579		
26.5	62.53	−13.61	2.064	.0596	−.0325		
27.0	63.03	−9.59	1.961	−.0019	−.0011		
27.6	63.62	−5.60	1.875	−.0465	−.0266		
28	64.01	−3.26	1.829	−.0675	−.0393		
28.5	64.48	−.59	1.780	−.0874	−.0520		
29.5	65.38	4.14	1.701	−.1142	−.0709		
30	65.82	6.27	1.668	−.1232	−.0782		
35	69.68	22.74	1.446	−.1489	−.1180		
40	72.83	34.42	1.314	−.1354	−.1349		
45	75.46	43.58	1.225	−.1136	−.1442		
50	77.73	51.15	1.160	−.0910	−.1500		
55	79.71	57.63	1.112	−.0700	−.1539		
60	81.49	63.34	1.077	−.0514	−.1566		
65	83.11	68.48	1.050	−.0357	−.1584		
70	84.61	73.21	1.030	−.0228	−.1598		
75	86.03	77.64	1.016	−.0128	−.1608		
80	87.38	81.87	1.007	−.0057	−.1614		
85	88.70	85.97	1.002	−.0014	−.1618		
90	90	90	-----	-------	---------	↓	↓

* These values apply for $x=0$ only. For $x=\infty$, values should be replaced by 0. All other values are independent of x.

TABLE I.—WAVE ANGLES AND TRANSFER FUNCTIONS—Continued

(i) $M=4.0$ ($m=4.57143$)

θ, deg	θ' deg	θ'', deg	S	Π	T	δ_s, deg	δ_T, deg
0	0	0	1.781	[a]1.6667	−0.4515	0	180.00
5	21.80	−5.33	1.795	[a]1.5269	−.4471	13.95	170.26
10	38.87	−10.65	1.837	[a]1.2248	−.4327	22.90	159.60
15	50.77	−15.95	1.917	[a].9087	−.4029	25.94	146.55
20	58.99	−21.22	2.059	[a].6107	−.3418	23.36	127.01
21.091	60.44	−22.36	2.106	[a].5444	−.3204	21.88	120.57
22.182	61.79	−23.50	2.164	[a].4760	−.2945	19.95	112.15
23.273	63.04	−24.64	2.251	[a].4090	−.2660	17.48	99.12
23.5	63.29	−24.88	2.280	[a].3978	−.2614	16.91	95.02
24.0	63.83	−25.40	2.411	[a].3972	−.2670	15.77	80.18
24.364 (θ_{cr})	64.22	−25.78	3.288	.6600	−.4515	0	0
24.370	64.22	−24.47	2.986	.4797	−.3281	↓	↓
24.400	64.26	−22.77	2.743	.3364	−.2303	↓	↓
24.404	64.32	−20.70	2.553	.2250	−.1545	↓	↓
24.500	64.36	−19.84	2.492	.1900	−.1306	↓	↓
24.564	64.42	−18.55	2.413	.1451	−.1001	↓	↓
24.664	64.53	−16.87	2.327	.0976	−.0676	↓	↓
24.750	64.62	−15.65	2.273	.0685	−.0476	↓	↓
24.764	64.63	−15.45	2.264	.0641	−.0446	↓	↓
25.000	64.87	−12.67	2.161	.0111	−.0078	↓	↓
25.250	65.12	−10.20	2.084	−.0256	−.0182	↓	↓
25.773	65.63	−5.95	1.971	−.0739	−.0539	↓	↓
27.182	66.93	2.64	1.790	−.1336	−.1038	↓	↓
28.591	68.13	9.22	1.676	−.1573	−.1303	↓	↓
30	69.25	14.70	1.591	−.1670	−.1474	↓	↓
35	72.65	29.37	1.394	−.1616	−.1792	↓	↓
40	75.39	39.94	1.274	−.1384	−.1940	↓	↓
45	77.66	48.24	1.192	−.1129	−.2025	↓	↓
50	79.60	55.07	1.135	−.0890	−.2078	↓	↓
55	81.29	60.92	1.093	−.0678	−.2115	↓	↓
60	82.80	66.06	1.063	−.0495	−.2140	↓	↓
65	84.18	70.68	1.041	−.0342	−.2158	↓	↓
70	85.45	74.94	1.024	−.0218	−.2171	↓	↓
75	86.65	78.92	1.013	−.0122	−.2180	↓	↓
80	87.79	82.71	1.006	−.0054	−.2186	↓	↓
85	88.90	86.38	1.002	−.0013	−.2189	↓	↓
90	90	90	-----	-------	---------	↓	↓

(j) $M=6.0$ ($m=5.26329$)

θ, deg	θ' deg	θ'', deg	S	Π	T	δ_s, deg	δ_T, deg
0	0	0	1.810	[a]1.6667	−0.5186	0	180.00
5	24.75	−5.14	1.827	[a]1.4906	−.5126	16.32	170.44
10	42.89	−10.28	1.879	[a]1.1422	−.4926	25.67	159.90
15	54.69	−15.41	1.980	[a].8059	−.4491	27.61	146.71
20	62.46	−20.52	2.163	[a].4878	−.3494	22.32	125.78
21	63.69	−21.55	2.216	[a].4164	−.3131	19.95	118.95
22	64.84	−22.57	2.282	[a].3360	−.2652	16.75	109.37
23	65.91	−23.59	2.412	[a].2590	−.2145	12.87	88.38
23.247 (θ_{cr})	66.16	−23.84	3.604	.6205	−.5199	0	0
23.250	66.16	−22.95	3.162	.4074	−.3415	↓	↓
23.297	66.21	−20.14	2.646	.1602	−.1346	↓	↓
23.347	66.26	−18.62	2.511	.0969	−.0815	↓	↓
23.447	66.36	−16.39	2.373	.0342	−.0289	↓	↓
23.547	66.46	−14.66	2.291	−.0016	−.0013	↓	↓
23.647	66.56	−13.21	2.232	−.0267	−.0229	↓	↓
24	66.91	−9.11	2.096	−.0799	−.0693	↓	↓
25	67.85	−.03	1.896	−.1425	−.1298	↓	↓
27	69.57	9.83	1.690	−.1801	−.1804	↓	↓
30	71.80	21.20	1.514	−.1861	−.2141	↓	↓
35	74.83	34.49	1.340	−.1650	−.2396	↓	↓
40	77.25	44.17	1.233	−.1370	−.2523	↓	↓
45	79.25	51.77	1.161	−.1100	−.2597	↓	↓
50	80.95	58.05	1.111	−.0859	−.2644	↓	↓
55	82.43	63.40	1.075	−.0650	−.2677	↓	↓
60	83.75	68.11	1.050	−.0473	−.2700	↓	↓
65	84.94	72.34	1.032	−.0375	−.2716	↓	↓
70	86.05	76.23	1.019	−.0207	−.2728	↓	↓
75	87.09	79.87	1.010	−.0116	−.2737	↓	↓
80	88.08	83.34	1.004	−.0051	−.2742	↓	↓
85	89.05	86.70	1.001	−.0013	−.2745	↓	↓
90	90	90	-----	-------	---------	↓	↓

(k) $M=\infty$ ($m=6.00000$)

θ, deg	θ' deg	θ'', deg	S	Π	T	δ_s, deg	δ_T, deg
0	0	0	1.833	[a]1.6667	−0.5832	0	180.00
5	27.70	−5.00	1.853	[a]1.4503	−.5754	18.67	170.58
10	46.61	−10.00	1.918	[a]1.0602	−.5484	28.05	160.10
15	58.12	−15.0	2.045	[a].7105	−.4873	28.51	146.67
20	65.40	−20.0	2.280	[a].3637	−.3253	19.33	123.90
20.552	66.03	−20.55	2.317	[a].3140	−.2889	17.12	119.67
21.104	66.64	−21.10	2.357	[a].2557	−.2420	14.29	114.51
21.656	67.23	−21.66	2.401	[a].1810	−.1761	10.35	107.57
22.208 (θ_{cr})	67.79	−22.21	2.449	.0000	.0000	0	0
23.182	68.73	−4.93	1.971	−.1586	−.1665	↓	↓
24.156	69.61	2.45	1.822	−.1875	−.2064	↓	↓
25.130	70.44	8.09	1.721	−.1993	−.2301	↓	↓
26.104	71.21	12.78	1.643	−.2036	−.2464	↓	↓
27.078	71.94	16.85	1.579	−.2039	−.2586	↓	↓
28.052	72.63	20.47	1.525	−.2018	−.2680	↓	↓
29.026	73.28	23.72	1.479	−.1981	−.2756	↓	↓
30	73.90	26.69	1.438	−.1935	−.3819	↓	↓
35	76.61	38.83	1.287	−.1638	−.3021	↓	↓
40	78.77	47.74	1.192	−.1334	−.3127	↓	↓
45	80.54	54.76	1.130	−.1060	−.3190	↓	↓
50	82.04	60.54	1.087	−.0822	−.3232	↓	↓
55	83.34	65.48	1.058	−.0619	−.3260	↓	↓
60	84.50	69.82	1.037	−.0449	−.3281	↓	↓
65	85.56	73.73	1.023	−.0308	−.3295	↓	↓
70	86.53	77.31	1.013	−.0196	−.3306	↓	↓
75	87.44	80.66	1.007	−.0109	−.3313	↓	↓
80	88.32	83.86	1.003	−.0048	−.3318	↓	↓
85	89.16	86.96	1.001	−.0012	−.3321	↓	↓
90	90	90	-----	-------	---------	↓	↓

[a] These values apply for $x=0$ only. For $x=\infty$, values should be replaced by 0. All other values are independent of x.

413072—57——46